Adapting a Fluorescence-Based Superoxide Detection Method in order to Visualize ROS in the Foliar Mitochondria of *Arabidopsis thaliana*

Allison McGuire
42029
allison.mcguire@abo.fi

Master's Thesis

Åbo Akademi University
Department of Biosciences
Faculty of Science and Engineering
29.05.2019

Specialization Theme: Cross-talk Between Light Acclimation and Defense Reactions in Plants (FCoE project)
Credits: 40 ECTS

Supervisors:
1: Sara Alegre García, Ph.D. Student

2. Jesús Pascual Vázquez, Postdoctoral Researcher

3. Saijaliisa Kangasjärvi, Ph.D.

Examiners:
1:

2:

Passed:

Grade:

ÅBO AKADEMI UNIVERSITY

Department of Biosciences

Faculty of Science and Engineering

Allison McGuire: Adapting a Fluorescence-Based Superoxide Detection Method in order to Visualize ROS in the Foliar Mitochondria of *Arabidopsis thaliana*

Biomedical Imaging

Master´s Thesis

Cross-talk Between Light Acclimation and Defense Reactions in Plants

May 2019

Abstract

Introduction: Plants are subjected to a variety of environmental stressors and must quickly acclimate to the prevailing conditions in order to survive and propagate. Many of the molecules and signaling pathways involved in stress response interact and overlap, complicating research into the mechanisms. The signaling pathways involving Reactive Oxygen Species (ROS) and the enzyme ALTERNATIVE OXIDASE 1A (AOX1A) are particularly useful in the study of environmental stress as related to Mitochondrial Retrograde Regulation. ROS are ubiquitous mitochondrial metabolic by-products, however, excessive concentrations of ROS can be damaging to plant tissue. To maintain homeostatic ROS levels, plants carefully regulate the production of the antioxidant enzyme, AOX1A, which dissipates ROS into heat and water. After stress exposure, plant signaling pathways initiate a recovery and acclimation phase. During recovery, mitochondrial retrograde signaling recruits the trimeric holoenzyme PROTEIN PHOSPHATASE 2A, and specific to this study, the isoform PP2A-B'γ, as a negative regulator of AOX1A. In order to bring the redox state of the cell back into balance, evidence suggests that PP2A-B'γ interacts with the mitochondrial metabolic enzyme ACONITASE 3 (ACO3), resulting in the dissipation of AOX1A.

Objectives: The purpose of this Master's Thesis is to determine how ROS-responsive fluorescent labeling might be used to study the negative regulation of AOX1A by PP2A-B'γ during UV-B induced stress signaling in the foliar mitochondria of *Arabidopsis thaliana*.

Methods: ROS production in Wild type and mutant *A.thaliana* plants was induced by chemical or UV-B treatment. Then, leaf samples were labeled with fluorescent probes designed to tag specific mitochondrial ROS molecules and imaged using Laser Scanning Confocal microscopy (LSM).

Results: Autofluorescent cell components confounded imaging attempts.

Keywords: ACO3, AOX1A, Crosstalk, PP2A-B'γ, Mitochondrial dysfunction, Mitochondrial retrograde regulation, ROS

List of Abbreviations

2-OH-E	2-Hydrooxyethidium
AA	Antimycin A
ACO3	Aconitase hydratase 3. Other names: mACO1, Citrate hydro-lyase 3
AOX	Alternative Oxidase
AOX1A	Alternative Oxidase 1A
aox1a	Alternative Oxidase 1A antisense/silenced mutant
ATP	Adenosine Triphosphate
DHE or HE	Dihydroethidium, Hydroethidine
DNA	Deoxyribonucleic Acid
ETC	Electron Transport Chain
GaAsP	Gallium Arsenide Phosphide
GMO	Genetically Modified Organism
H_2O_2	Hydrogen Peroxide
2-OH-E	2-Hydroxyethidium
MQ	Milli-Q Deionized water
NO	Nitric Oxide
O_2^-	Superoxide
PP2A	Protein Phosphatase 2A
PP2A-B'γ	Protein Phosphatase 2A Regulatory Subunit B'γ
pp2a-b'γ	Protein Phosphatase 2A Regulatory Subunit B'γ knock-down mutant
PMT	Photomultiplier Tube
PPFD	Photosynthetic Photon Flux Density
ROS	Reactive Oxygen Species

RT	Room Temperature
SHAM	Salicylhydroxamic Acid
UV-B	Ultraviolet, Shortwave Ultraviolet
WT	Wild Type

Table of Contents

1. Introduction

1.1. Plant Cell Stress Response is Conditional

In order to survive as sessile organisms, plants have developed numerous, complex, and interconnected strategies capable of detecting environmental stressors and unleashing rapid defense responses in order to contend with unfavorable growing conditions. The source of environmental stress is categorized as either biotic or abiotic. Biotic stressors include pathogen infection and insect phytophagy, while abiotic stressors encompass conditions such as drought, soil salinity, extreme temperatures, excess light, and UV exposure (Lichtenthaler, 1995; Rahikainen, 2018). In nature, these environmental stressors often present concurrently; for example, a period of drought is likely to accompany excessive light conditions. Previous research has revealed that the defense responses produced by plants are dependent on the prevailing combination of environmental stresses in tandem with the duration of exposure to those stresses (Mittler, 2006; Rizhsky et al., 2004). Subsequently, the resulting molecular and metabolic profiles generated in response to environmental stress are unique, suggesting that plants elicit a specific and targeted response against each type of stress. However, further investigation reveals this is not entirely accurate.

Confoundingly, even though each response is specialized and condition-dependent, plants actually recruit many of the same organelles, signaling pathways, transcription factors, and molecular components (Atkinson & Urwin, 2012; Foyer, Rasool, Davey, & Hancock, 2016; Knight & Knight, 2001). By utilizing common elements, plants initiate a relatively generic defense response, thereby conserving resources and energy. Nonetheless, plant cell signaling components have proved to be remarkably multipurpose, lending flexibility and specificity to the otherwise broad cellular response. This inherent plasticity of plant signaling mechanisms contributes to the phenomenon of crosstalk in plant defense signaling, wherein plants that have recovered from abiotic stress exposure are shown to be more resilient against subsequent exposure to biotic stressors (Knight & Knight, 2001; Rejeb, Pastor, & Mauch-Mani, 2014; Trotta, Rahikainen, Konert, Finazzi, & Kangasjärvi, 2014). In stress signaling pathways, biomolecules at each step have the potential to interact with, regulate, and/or transduce signals to other cellular components in a concerted effort to restore homeostasis. Consequently, understanding plant stress defense depends on untangling the convoluted

molecular interactions where factors such as molecular concentration, timing, and localization play a crucial role in determining the characteristics of the stress response and the final outcome.

1.2. Environmental Stress Conditions Can Be Artificially Reproduced in Laboratory Settings

As expected, the plasticity of plant cell signaling presents numerous challenges to researchers seeking to examine the defense responses of plants. Because the plant stress response is dose dependent, the type of environmental stressor and the duration of exposure must be controlled for. In a laboratory setting, such conditions can be replicated by exposing plant tissue to chemical agents or by altering the conditions of the growing environment.

1.3. The Model Organism Arabidopsis thaliana is used in Plant Stress Research

In abiotic stress studies, *Arabidopsis thaliana*, henceforth *A. thaliana*, is widely used as a model organism as its genome sequence is publicly accessible and mutant variations can be purchased or transformed, and even propagated relatively easily. Figure 1 illustrates the general appearance, size, and growth pattern of wild type *A.thaliana* plants grown in laboratory settings. A member of the Brassicaceae family, *A. thaliana* is characterized by a compact size, short life cycle, and the ability to self-pollinate; ideal characteristics for use in laboratories where time and space are valuable resources (Koornneef & Meinke, 2010).

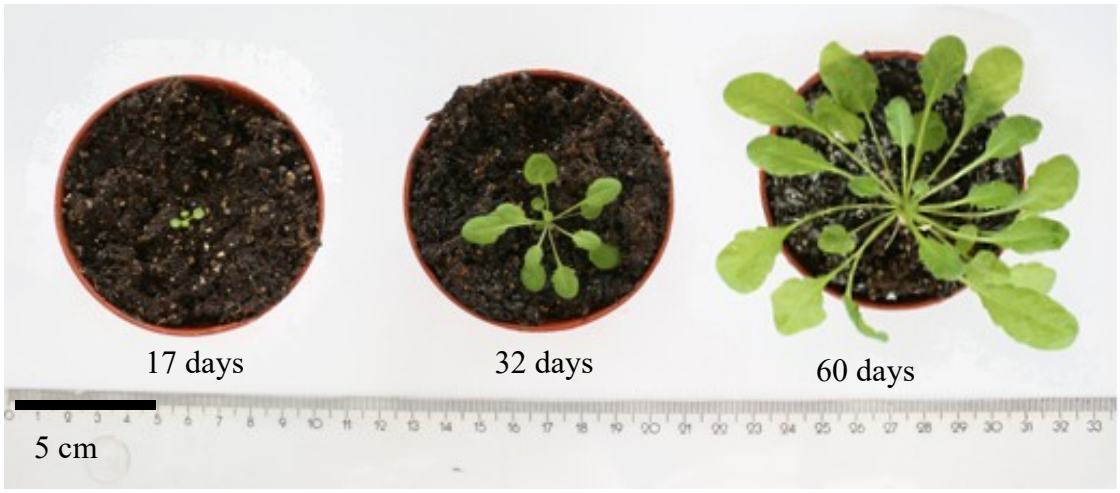

Figure 1: Composite photo of different wild type *A. thaliana* plants showing progressive stages of growth at approximately 2 weeks (17 days), 5 weeks (32 days), and 8 weeks (60 days) old, respectively.

1.4. UV-B Radiation Treatment Induces an Abiotic Stress Response

In order to mimic the effects a changing climate might have on growing conditions, stress response studies routinely expose *A. thaliana* to "excessive" or "high" light stress and ultraviolet radiation (UV-B) (Nawkar et al., 2013). Both light intensity and UV-B radiation exposure can be precisely controlled for and reproduced in laboratory conditions. Light intensity is expressed in terms of photosynthetic photon flux density (PPFD) and for *A. thaliana*, values in excess of 600-700 µmol photons $m^{-2}s^{-1}$ are categorized as excessive (Eckardt, Snyder, Portis, Orgen, & Orgen, 1997). Likewise, high doses of UV-B radiation are defined as values above the ambient level; in plant research, a dose may fall between 1–3 µmol photons $m^{-2}s^{-1}$ (Brown & Jenkins, 2008; Müller-Xing, Xing, & Goodrich, 2014). Though an intrinsic component of high light, the specific effects of UV radiation alone are still under study. Acute exposure to simultaneous high light stress and UV-B radiation appear to affect the balance of oxidative and reductive states in the metabolic organelles of plant cells: the chloroplasts and mitochondria (Brown & Jenkins, 2008; Müller-Xing et al., 2014).

1.5. Chloroplasts, Mitochondria, and the Formation of Reactive Oxygen Species (ROS)

1.5.1. Abiotic Stress Drives the Excessive Production of ROS

Arguably, chloroplasts play a primary role in environment sensing and are fundamentally involved in both stress detection and initiating the response. However, mitochondria are likewise essential metabolic operators necessary for the transformation of light energy into adenosine triphosphate (ATP), which provides the chemical energy needed to drive cellular functions. In addition to ATP, aerobic metabolism also produces Reactive Oxygen Species (ROS) as a byproduct (Møller, 2001). In general, these oxygen containing compounds are chemically active oxidizing agents such as hydrogen peroxide (H_2O_2), superoxide (O_2^-), and nitric oxide (NO) (Foyer, Leiandais, Foyer, Leiandais, & Kunert, n.d.; Møller, 2001). When subjected to high light levels, chloroplasts absorb an excess of excitation energy, which increases the concentration of reducing agents and leads to increased levels of ROS formation in both the chloroplasts and the mitochondria (Foyer & Noctor, 2003; Konert, 2014; Vishwakarma, Bashyam, Senthilkumaran, Scheibe, & Padmasree, 2014). Excessive concentrations of ROS can be detrimental to the cell. ROS cause oxidative damage to DNA, proteins, and lipids, and eventually, ROS accumulation can result in cell death (Møller, 2001). Paradoxically, though toxic, ROS are found ubiquitously in plant tissue and are produced by many cellular compartments (Konert et al., 2014; Rizhsky et al., 2004). Thus, in order to preserve cellular integrity, ROS levels must be delicately maintained within the cell. This oxidative modulation is achieved by the upregulation of various antioxidizing metabolites in response to increased ROS (C. J. Baxter et al., 2007). Therefore, it seems appropriate that ROS also function as key signaling molecules within this regulatory pathway (A. Baxter, Mittler, & Suzuki, 2014).

1.5.2. ROS Act as Signaling Molecules

Redox signaling in plants involves numerous metabolic interactions between the cytoplasm, chloroplasts, and mitochondria. For example, metabolic intermediates can be shuttled between the chloroplasts and the mitochondria in the cytoplasm (Igamberdiev & Eprintsev, 2016; Rahikainen, 2018). Some of these redox signals are intercepted by

other cytoplasmic signaling networks where they can provoke responses in still other cellular compartments, particularly in the nucleus. Cell messaging from the organelles to the nucleus is termed “retrograde signaling” or “retrograde regulation” (Liao & Butow, 1993). In this manner, ROS concentration vicariously initiates nuclear gene expression and influences the post-translational modification of enzymes.

1.5.3. Fluorescent Probes are used to Study ROS

Accordingly, in order to study retrograde regulation, researchers must attempt to capture and measure the concentrations of mitochondrial ROS. These applications and methods are as diverse as they are numerous, and span across the various scientific disciplines. The continued development of ROS-reactive fluorescent probes has given researchers the opportunity to microscopically visualize the localization of ROS within tissues, and even within certain organelles, in relation to various cell signaling events.

When labeling plant tissue for fluorescent microscopy, the natural abundance of autofluorescent compounds found within plant tissue cannot be disregarded. Amongst these compounds, chlorophyll is one of the most apparent due to its pervasive nature (Goodwin, 1953). The autofluorescent quality of chlorophyll, and thus chloroplasts, is an intrinsic feature of the photosynthetic mechanism (Zhou, Carranco, Vitha, & Hall, 2005). Since the emission spectra of many of these autofluorescent compounds overlap with commercially available fluorescent probes, the choice of applicable probes is greatly limited. Two such probes that accommodate these criteria are the mitochondrial probes MitoSOX™Red and MitoTracker™ Orange CMTMRos

1.5.4. MitoSOX™ Red

MitoSOX™Red (henceforth referred to as MitoSox), is a fluorescent probe derived from ethidium bromide. Non-fluorescent dihydroethidium (also known as hydroethidine, HE, and DHE) oxidizes into strongly fluorescent 2-Hydroxyethidium (2-OH-E) upon chemical interaction with superoxide, O_2^- (Zhao et al., 2003). In order to target the ROS specifically in the mitochondria, DHE is conjugated to the triphenylphosphonium moiety which causes electrical potential-driven accumulation of DHE in the mitochondria (Bakeeva et al., 1970; Robinson et al., 2006). On these principles, MitoSox is often employed as a qualitative measure of superoxide presence,

though its use as a quantitative tool is heavily disputed (Benov, Sztejnberg, & Fridovich, 1998). Caveats for use of the probe include sensitivity to air and light, auto-oxidation, and, in high concentrations (>5 μM), labeling of the nucleus and cytosol (Dikalov & Harrison, 2014; "MitoSOX Red Mitochondrial Superoxide Indicator, for live-cell imaging - Thermo Fisher Scientific," n.d.).

MitoSOX™ Red Mitochondrial Superoxide Indicator for live-cell imaging	
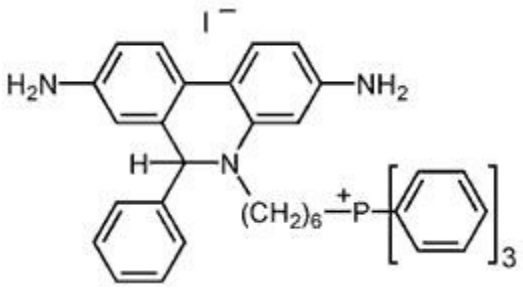	Molecular formula: $C_{43}H_{43}N_3IP$ Molecular weight: 759.71

Figure 2: Chemical structure of MitoSox.
("MitoSOX Red Mitochondrial Superoxide Indicator, for live-cell imaging - Thermo Fisher Scientific," n.d.,)

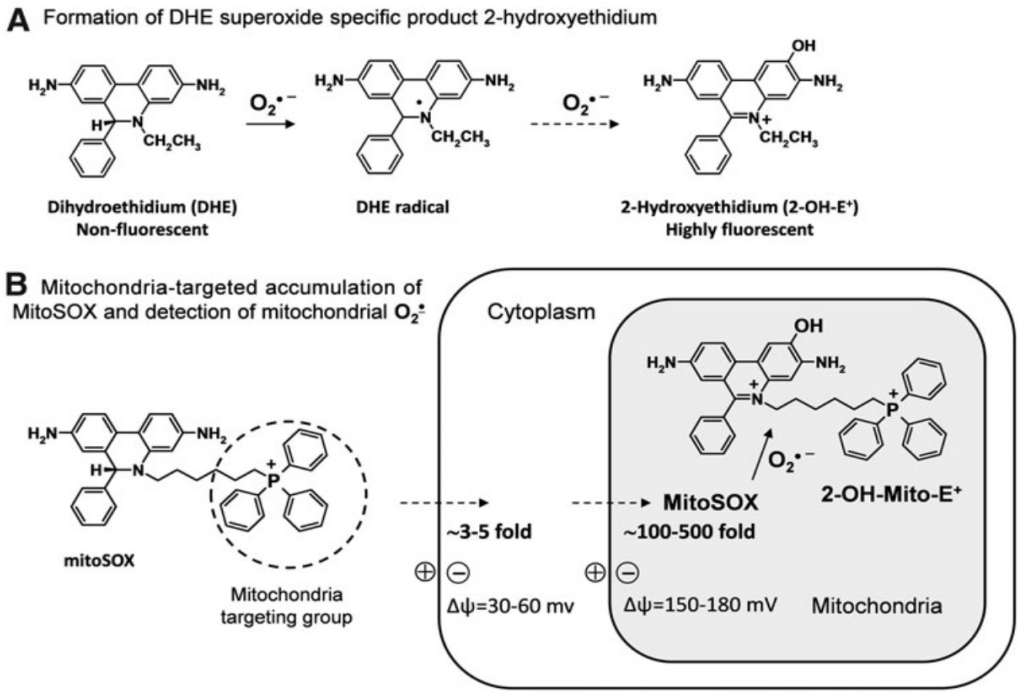

Figure 3: A. The formation of fluorescent product 2-OH-E upon chemical interaction of DHE with superoxide, O_2^-.
B. Diagram of the electrical potential driven uptake and retention of MitoSox in the Mitochondria. (Image from Dikalov & Harrison, 2014).

1.5.5. MitoTracker™ Orange CMTMRos

Though not a ROS-reactive probe, MitoTracker™ Orange CMTMRos (henceforth MitoTracker) labels mitochondria by a similar mechanism to MitoSox, but exhibits fluorescence irrespective of superoxide concentrations. For this reason, MitoTracker is used in tandem with MitoSox as a positive labeling control. MitoTracker contains an alkylating chloromethyl moiety which drives electrical potential-driven accumulation of the probe across the mitochondrial membrane (Poot et al., 1996). The probe is then sequestered in the mitochondria through the formation of covalent bonds with mitochondrial protein thiols ("Dihydroethidium (Hydroethidine) - Thermo Fisher Scientific," n.d.; Poot et al., 1996). MitoTracker labeling is retained even if membrane potential is later lost, for example, due to sample fixation ("Dihydroethidium (Hydroethidine) - Thermo Fisher Scientific," n.d.; Poot et al., 1996). Caveats of the use of this probe include sensitivity to light and air ("Dihydroethidium (Hydroethidine) - Thermo Fisher Scientific," n.d.).

MitoTracker™ Orange CMTMRos	
	Molecular formula: $C_{24}H_{24}Cl_2N_2O$ Molecular weight: 427.37

Figure 4: Chemical structure of MitoTracker Orange.
("MitoTracker Orange CMTMRos - Special Packaging - Thermo Fisher Scientific," n.d,)

1.6. Research on Mitochondrial Dysfunction Response Exposits Mitochondrial Retrograde Signaling

In addition to using fluorescent probes, researchers attempt to track the retrograde signals that spawn directly from the mitochondria by subjecting specimens to genetic and stress-related conditions in which the normal function of the mitochondria is

significantly impaired. By studying this "mitochondrial dysfunction response," researchers have identified the upregulation of ALTERNATIVE OXIDASE (AOX) to be a well-established indicator of mitochondrial retrograde regulation (Vanlerberghe & McIntosh, 1997; Zarkovic, Anderson, & Rhoads, 2005).

As the name suggests, the ALTERNATIVE OXIDASE enzyme provides an alternative route for electrons to bypass the electron transport chain in plant mitochondria (Maxwell, Wang, & McIntosh, 1999). Like the cytochrome respiratory pathway, AOX is also located in the mitochondrial membrane (Maxwell et al., 1999). However, when electron flow is diverted through AOX, molecular oxygen is reduced to water and heat is generated without producing ATP (Moore & Siedow, 1991). Thus, when ROS production escalates during stress exposure, electron flow is diverted from the electron transport chain and ROS, namely O_2, is dissipated by AOX activity in the mitochondria (Vishwakarma et al., 2014).

In *A.thaliana* stress response studies, the increased expression of the AOX isoform AOX1A is of particular interest. The upregulation of AOX1A is known to be routinely induced by numerous environmental stress conditions related to mitochondrial dysfunction (Vanlerberghe & McIntosh, 1997). Additionally, its function cannot be fully compensated by the other four known AOX isoforms, AOX1B-AOX1D and AOX2 (Selinski et al., 2018).

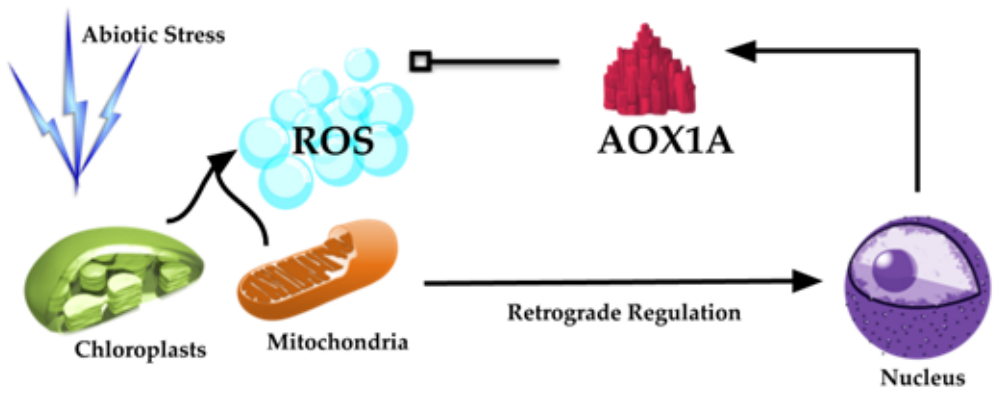

Figure 5: Abiotic stress exposure results in increasing concentrations of ROS in the chloroplasts and mitochondria. Signals from the mitochondria to the nucleus initiate the transcription of stress response enzymes like AOX1A. The resulting AOX1A enzymes then downregulate ROS. (Diagram adapted from Vanlerberghe & McIntosh, 1997.)

1.7. PP2A-B'γ as a Negative Regulator of Stress Response

Emerging work in plant stress defense also seeks to explore the role of post translationally modified enzymes in the regulation of ROS. One mechanism of interest is protein phosphorylation, as mediated by protein kinases (adds a phosphate group) and protein phosphatases (removes a phosphate group). Because phosphorylation alters the structure of the enzyme, it also affects enzymatic activity. Though not as well characterized as their kinase counterparts, protein phosphatases are highly conserved in eukaryotic organisms due to their undeniable role in stress defense, particularly those in the protein phosphatase sub-family Protein Phosphatase 2A (PP2A) (Konert et al., 2014; Moorhead, De Wever, Templeton, & Kerk, 2009; Rahikainen, Pascual, Alegre, Durian, & Kangasjärvi, 2016). Structurally, PP2A is a trimeric holoenzyme consisting of a scaffolding subunit A, a catalytic subunit C, and a regulatory subunit B (Cho & Xu, 2007). In eukaryotes, each PP2A subunit may be encoded by several different genes, giving rise to numerous possible structural combinations. Investigation of PP2A reveals that subunit B contains the binding sites which determine substrate specificity. In *A. thaliana*, 17 genes encode for the regulatory B subunit and are further categorized as B, B′, and B′′ (Rahikainen et al., 2016; Trotta et al., 2011).

Reverse genetic screenings identified the enzyme complex PP2A-B'γ as a potential modulator of redox regulation due to the abnormal phenotype of the *pp2a-b'γ* knockdown *A. thaliana* mutant (Trotta et al., 2011). According to Trotta et al., the *pp2a-b'γ* phenotype exhibits stunted growth, wrinkled leaves, delayed flowering, and the age-dependent formation of yellowing lesions, despite being grown under moderate light intensity (2011). Follow-up with proteomic analyses in the leaves indicated that elevated levels of foliar ROS are likely responsible for the early senescence and physical abnormalities of the phenotype (Li, Mhamdi, Trotta, Kangasjärvi, & Noctor, 2014; Trotta et al., 2011).

Previous experiments on *pp2a-b'γ* in *A. thaliana* indicate that PP2A-B'γ negatively regulates antioxidant activity and controls ROS signaling, thereby promoting cellular ROS homeostasis, mitigating unnecessary stress responses, and facilitating stress recovery and acclimation (Rahikainen et al., 2016). In 2014, Konert *et al*., employed a battery of proteomic experiments in *pp2a-b'γ* mutants, the results of which suggest a correlation between ROS, PP2A-B'γ, and diminished AOX concentrations (namely

isoforms AOX1A and AOX1D). In order to further understand this relationship, current research seeks to identify other stress response enzymes that interact with PP2A-B'γ. One such candidate is ACONITASE 3 (ACO3) (Konert et al., 2014).

ACO3 is characterized as an enzyme that is integrally connected to mitochondrial metabolism reactions and the electron transport chain (Konert et al., 2014). Structurally, ACO3 contains a $[4Fe\text{-}4S]^{2+}$ cluster, making it vulnerable to oxidative inactivation by ROS (Verniquet, Gaillard, Neuburger, & Douce, 1991). Consequently, during stress, ACO3 inhibition provokes an upregulation of AOX1A gene expression (Gupta et al., 2012; Konert, 2014). But, as previously discussed, mounting a continuous stress defense would toll heavily against a plant's available resources. Since previous studies suggest that ACO3 and PP2A-B'γ co-localize in the cytoplasm, this interaction might allow the plant to acclimatize, re-divert resources, and recover from stress (Konert et al., 2014). Therefore, the dephosphorylation of ACO3 by PP2A-B'γ, could be a potential mechanism that quenches the upregulation of AOX constituents and mediates stress recovery, as illustrated by Figure 6 (Konert, 2014; Pascual et al., unpublished data).

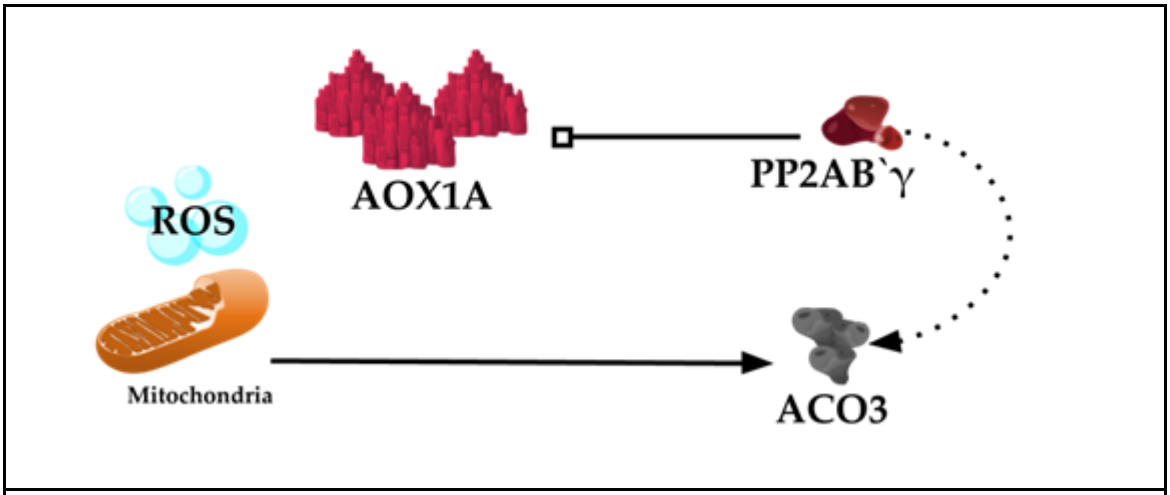

Figure 6: A potential mechanism by which AOX1A is down regulated during stress recovery: PP2A-B'γ dephosphorylates ACO3 which then quenches the upregulation of AOX1A.

1.8. The Effects of UV-B Radiation in Relation to PP2A-B'γ is Beneficial to Study

In review, plant cell stress response is conditional and dose-dependent. Therefore, even though stress pathways share numerous common elements, the ultimate profile of the response is specific and unique. Similarly, extrapolating upon the phenomenon of crosstalk in plant defense could eventually be applied to improve the survivability and cultivation of numerous higher plant species. Thus, it is beneficial to investigate the molecular and metabolomic profiles generated by specific stress conditions, such as UV-B radiation. Though the effects of UV-B radiation appear to be similar to those caused by other abiotic stressors, prior investigations suggest that there is still much to be discovered.

Presently, the Molecular Plant Biology lab of Dr. Saijaliisa Kangasjärvi studies "Light Acclimation and Defense Reactions in Plants" where the lab group, and their collaborators, are interested in the relationship between abiotic stress and ROS accumulation in the organelles and how their effects manifest in the phenotype of plants. By investigating the function of PP2A-B'γ as a negative regulator of AOX1A after stress exposure, this Master's Thesis seeks to give a more complete understanding of the signaling pathways that connect environmental stress, ROS accumulation, and mitochondrial retrograde signaling.

2. Aims

The purpose of this Master's Thesis was to determine if ROS molecules accumulate in the foliar mitochondria of stressed *pp2a-b'γ* in significant concentrations as compared to a stressed wild type (WT), and potentially, as compared to stressed overexpressor mutants.

The specific aims were as follows:

1. To implement a protocol to fluorescently tag and image the ROS molecule O_2^- in the mitochondria of *pp2a-b'γ A. thaliana* leaf tissue.

2. To calibrate and quantify the strength of the resulting fluorescent signal in a way that could be correlated to mitochondrial O_2^- abundance.

3. To compare fluorescent signal strength/relative abundance of O_2^- between stressed and unstressed WT and mutant varieties.

3. Experimental Design

This project followed the experimental design implemented by Cvetkovska & Vanlerberghe in 2012, wherein the leaves of mutant strains of tobacco plants, *Nicotiana tabacum,* were fluorescently tagged with MitoSOX™ Red and imaged with a confocal microscope. In their study, image analysis of the resulting micrographs provided a method for comparing mitochondrial ROS accumulation within live cells. For study purposes, modifications were made to the original protocol as necessary, in a bid to adapt the technique for use in wild type and mutant *A. thaliana* plants. The original experiment was further expanded to include fluorescently labeling and imaging both stressed and unstressed plants, as well as protoplasts.

4. Workflow

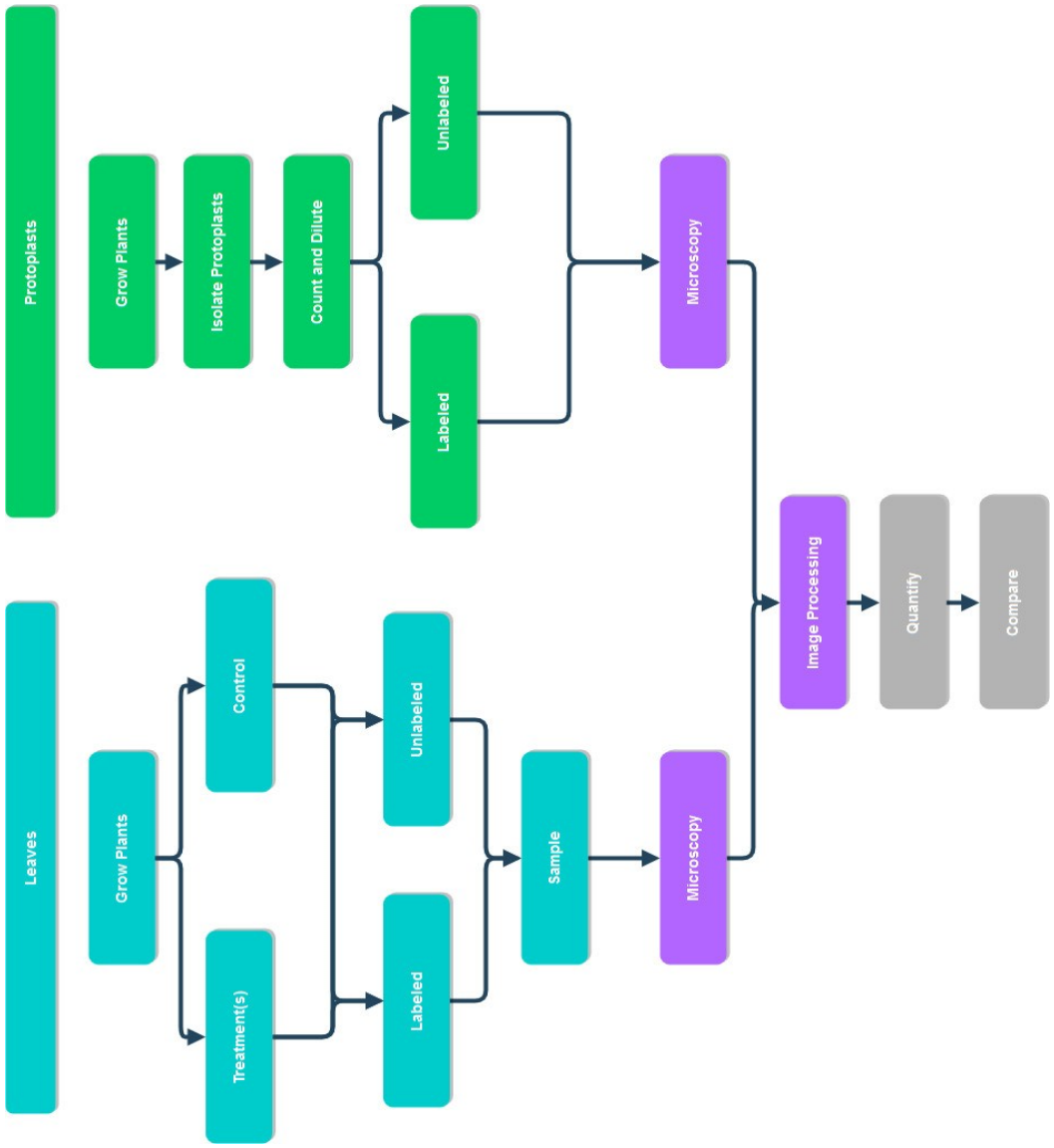

Figure 7: A flowchart of the planned protocol. Note that the Quantification and Comparison steps could not be accomplished during the course of this thesis project.

5. Hypotheses

Null hypothesis: Fluorescent signal strength in the mitochondria of *pp2a-b'γ A. thaliana* mutants will show no statistically significant difference between WT and mutant varieties.

Hypothesis: Fluorescent signal in the mitochondria of *pp2a-b'γ* will be more prevalent than signal generated in WT and overexpressor mutants.

6. Materials and Methods

6.1. Plant Mutants and Accession Information

During the course of this thesis work, both *A. thaliana* and *Nicotiana benthamiana* plants were utilized. *A. thaliana* is used in many plant stress studies as the genome is publicly available and mutant lines can be purchased, transfected, and even propagated if possible. Wild type *N. benthamiana* was simply used in order to compare the implementation of the modified protocol against that of the original. Table 1 indicates the varieties of *A. thaliana* involved, including the homozygotic knockdown mutation of *pp2a-b'γ*, the overexpressor line COMP, and a mis-sense *aox1a* mutant. Mutant lines were supplied by the Plant Molecular Biology lab of Dr. Saijaliisa Kangasjäarvi, currently licensed by the Finnish Gene Technology board for the growing and handling of class 2 GMOs.

Table 1: Accession information for experimental plant lines		
Wild Type:		*Arabidopsis thaliana* ecotype Columbia
Mutant lines:		
pp2a-b'γ	Knockdown	Homozygotic *pp2a-b'γ* (SALK_039172 for AT4G15415)
COMP	Overexpressor	*pp2a-b'γ* 35S::PP2A-B'γ
aox1a	Knockout	*aox1a* (Umbach, 2005)

Wild Type:	*Nicotiana benthamiana*

6.2. Growing Conditions

Seeds were potted in soil mixture composed of 3:1 general purpose soil to vermiculite. To stratify germination, seeds were placed in a cold room of 4°C, in darkness, for 72 hours. On Day 0, plants were moved into a short day phytotron with an 8 hour photoperiod, photosynthetic photon flux density of 130 µmol photons $m^{-2}s^{-1}$, daytime temperature of 22°C, and relative humidity of 50%. Plants were irrigated with water at regular intervals (every 2-3 days), and were allowed to grow for a minimum of 20 days before use.

6.3. Fluorescent Probe Specifications

In order to visualize and compare the production of ROS in foliar mitochondria, the following fluorescent probes were used:

Table 2: Fluorescent probe details and specifications

Probe Name	Description	Excitation	Detection
MitoSOX™Red (M36008; Invitrogen, Carlsbad, CA, USA)	Oxidation of MitoSOX™ Red reagent by superoxide produces red fluorescence.	488 nm (maxima: 510 nm)	588–615 nm (maxima: 580 nm)
MitoTracker™ Orange CMTMRos (M7510; Invitrogen, Carlsbad, CA, USA)	Orange fluorescent dye that stains mitochondria in live cells. Accumulation is dependent on membrane potential.	543 nm	553-606 nm

Despite the somewhat overlapping emission spectra of MitoSox and MitoTracker, these probes were used in a double labeling experiment to determine if the probes were being loaded successfully by the protocol. Since the optimal excitation lasers for each probe are different (MitoSox: 488 nm and MitoTracker Orange: 543 nm) and the detection range for each probe falls within the fluorescent emission valley for both chlorophyll A and B, it was reasoned using both labels would be sufficient for this purpose.

6.4. Treatments

Depending on the trial, treatment group plants were subjected to chemically induced stress and/or UV-B radiation.

UV-B radiation was administered by placing plants in a Weiss growth chamber containing a UV lamp. Plants were exposed to a dose of approximately 3 µmol photons $m^{-2}s^{-1}$ for 45 minutes.

Chemical treatment with Antimycin A (AA) (50uM AA in 0.01% Tween 20) was used as a positive control to increase the quantity of mitochondrial ROS available to interact with the MitoSox probe. Antimycin A is a nonlethal treatment known to inhibit electron transport at mitochondrial complex III, which activates mitochondrial retrograde response genes and exacerbates ROS production in the mitochondria (Maxwell et al., 1999; Vanlerberghe & McIntosh, 1997).

Antimycin A	
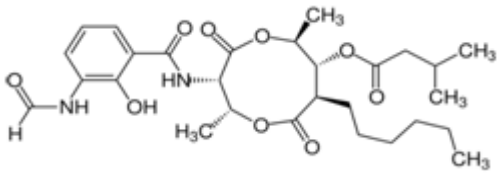	Chemical formula: $C_{28}H_{40}N_2O_9$ Molar mass: 548.633 g·mol^{-1}
Figure 8: The chemical structure of Antimycin A ("File:Antimycin A1 Structural Formula V1.svg - Wikimedia Commons," n.d.)	

Similarly, chemical treatment with salicylhydroxamic acid (SHAM) (10 mM SHAM in 0.1% DAB) was used as a positive control because it prevents the binding of oxygen by the AOX enzyme, thus preventing AOX from eliminating available ROS (Rasool et al., 2014; Schonbaum, Bonner, Storey, Bahr, & Bahr, 1971).

Salicylhydroxamic Acid (SHAM)	
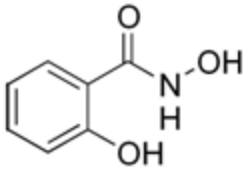	Chemical formula: $C_7H_7NO_3$ Molar mass: 153.137 g·mol^{-1}
Figure 9: The chemical structure of SHAM ("File:Salicylhydroxamic acid.png - Wikimedia Commons," n.d.)	

6.5. Confocal Laser Scanning Microscopy Specifications

Images were acquired using a confocal Carl Zeiss LSM880 AiryScan inverted microscope equipped with the following hardware:

Excitation Lasers	
405 nm	561 nm
458,488,514 nm	633 nm

Table 3: Zeiss LSM880 AiryScan Confocal Microscope Specifications	
Objectives	
Plan-Apochromat 10x/0.30 M27, WD 2.000mm	
Plan-Apochromat 20x/0.8 M27, WD 0.550mm	
LD LCI Plan-Apochromat 40x/1.2 Imm Corr W/glycerol/silicon oil DIC M27, WD 0.410mm	
C Plan-Apochromat 63x/1.4 Oil DIC UV-VIS-IR M27, WD 0.140mm	
alpha Plan-Apochromat 100x/1.46 Oil DIC, WD 0.110mm	
Detectors	
Photomultiplier Tube (PMT)	Cooled PMT
Airy Scan detector	Gallium Arsenide Phosphide (GaAsP) element detector

The accompanying software package version was Zen Black 2.3 SP1. Microscopes and support services were provided by the Turku Center for Biotechnology Cell Imaging Core.

Due to the reactive nature of ROS, images needed to be acquired from freshly harvested samples. As previously mentioned, plants naturally contain a variety of autofluorescent compounds, like chlorophyll, which are stimulated by many of the same laser lines as fluorescent probes (*Product Info: Fluorescent probes for plant imaging Invitrogen tools for plant cell biology*, n.d.). Therefore, imaging plant material is inherently challenging. Autofluorescence can generate background signal, noise, and can even interfere with the levels of detectable signal from fluorescent probes/stains/dyes (Kodama, 2016; Zhou et

al., 2005). Additionally, leaf tissue samples tend to be thick (~100µm), and the individual cells themselves are difficult to distinguish as they are interlocked in a three-dimensional mosaic (Kalve, Fotschki, Beeckman, Vissenberg, & Beemster, 2014).

For this project, the Zeiss LSM 880 with AiryScan modality was selected because this particular microscope setup offered the necessary excitation lasers as well as the ability to specifically select the signal detection range, while maintaining a relatively quick scan time suitable for live cell imaging. The ability to choose the specific detection range was a crucial component of this project, as the probes being used as well as the natural autofluorescent compounds had some overlap in their emission ranges.

Additionally, this microscope combines the principles of confocal microscopy with the flexibility of point-by-point laser scanning. Confocality is achieved through the use of an adjustable pinhole where the size of the pinhole limits the amount of laser light that can be detected to only light captured from the focus plane (Nicolas George, 2004). This feature makes it possible to image within the mesophyll layer of a plant leaf, despite a thick tissue sample.

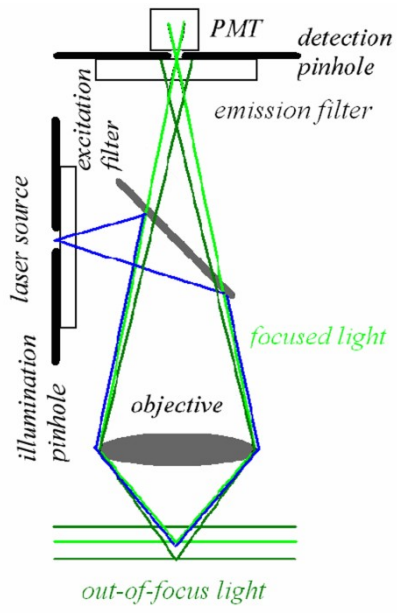

Figure 10: Light path diagram of multi-photon excitation confocal microscopy (Diaspro et al., 2006).

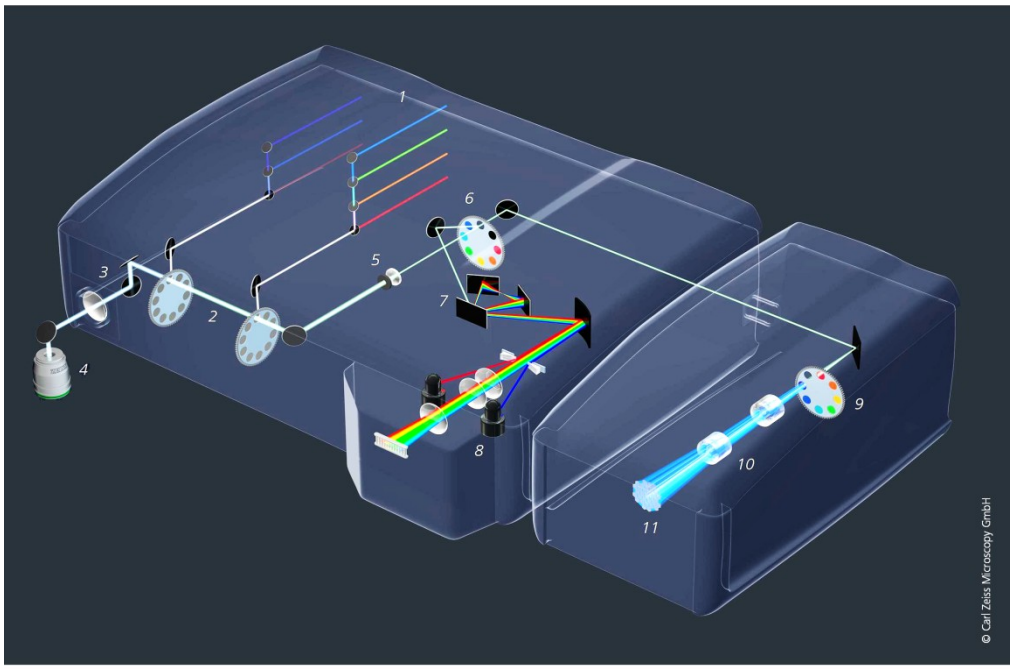

1. Excitation laser lines 2. Twin Gate main beam splitters 3. Galvo scanning mirrors' 4. Objective 5. Pinhole and pinhole optics 6. Secondary beam splitters	7. Recycling loop 8. Quasar detection unit 9. Emission filters 10. Zoom optics 11. Airyscan detector

Figure 11: Diagram of the beam Path of the Zeiss LSM880 with Airyscan ("File:ZEISS LSM 880 with Airyscan (14657209838).jpg - Wikimedia Commons," n.d.)

6.6. Spectral Imaging and Linear Unmixing

One method used to separate autofluorescent signal from detection of the desired probes in plant tissue is the application of spectral imaging and linear unmixing. With this function, specific detectors, in cooperation with mathematical algorithms, can be used to distinguish probes with overlapping emissions. The unmixing calculation is simplified as:

$$S(\lambda) = \sum \mathrm{A} * \mathrm{R}(\lambda)$$

Where the weight (A) of each fluorophore reference spectrum R(λ) equals the measured spectrum $S(\lambda)$ (Dickinson & Davidson, n.d.-a).

The LSM880 is equipped with a 32 channel Quasar detection unit which captures intensity information for the fluorophore within a 10 nm bandwidth, known as a lambda stack. After building a lambda stack from individually labeled samples, by comparing the calculated pixel intensity information for each detection parameter in the lambda stack, the software can separate out the most probable emission signature for each fluorophore and then apply them to subsequent, similarly captured images labeled with the overlapping fluorophores (Dickinson & Davidson, n.d.-b).

6.7. Image Analysis Software

All resulting images were processed in Zen Black 2.3 SP1, Zen lite 2.3 (Zen Blue), and/or ImageJ 1.52n.

6.8. Protoplast Isolation

In order to determine if the plant cell wall hindered the loading of the mitochondrial probes, protoplast isolation was performed according to the protocol established in 2009 by Fu-Hui Wu *et al.*

6.9. Procedure

6.9.1. Assess Applicability of Protocol for Use in *A. thaliana* Leaves

In order to determine the viability of the Cvetkovska & Vanlerberghe 2012 protocol in *A. thaliana*, several groups of plants consisting of both WT and mutants, were processed. Attempts were also made to determine the most appropriate probe delivery method, concentration, and incubation times. Samples were then mounted to microscope slides and the mesophyll cell layer was imaged on the LSM880 confocal microscope with the appropriate excitation and detection settings and filters. Sample

fixatives were not applied due to the reactive nature of ROS. Acquisition settings were adjusted as necessary. In order to establish an autofluorescence baseline, unlabeled leaf segments from each of the experimental and control plant groups were also imaged with the same acquisition settings.

The most recent adaptation of the Cvetkovska & Vanlerberghe 2012 protocol, though not adequately optimized, is as follows:

Established *A. thaliana* plants (minimum 30 days old) were divided into experimental and control groups and subjected to their respective treatments. Next, a few fully opened leaves of the selected plants were infiltrated with a 5 µM solution of MitoSOX™Red in Milli-Q deionized water (MQ) delivered via 1 mL needleless plastic syringe, in darkness, at room temperature, 30 minutes prior to imaging. Infiltrated leaf tissue was then sampled with a cork borer, mounted to microscope slides with MQ water, topped with a coverslip, and secured with adhesive tape. For double labeling experiments, a 1 µM solution of MitoTracker™ Orange CMTMRos was similarly delivered. Samples and slides were then appropriately discarded at the end of imaging.

6.9.2. Assess Applicability of Protocol for Use in *A. thaliana* Protoplasts

In order to determine if the plant cell wall hindered loading of the fluorescent probes, isolated protoplasts were processed, quantified and diluted. Dilutions were then loaded with a 5 µM solution of MitoSOX™ Red and/or a 1 µM solution of MitoTracker™ Orange CMTMRos, and incubated in darkness, at room temperature for 30 minutes prior to imaging with the LSM880.

7. Results

7.1. Autofluorescent Compounds Confound Imaging Attempts

The cumulative effect of prolonged stress defense may help to explain the unusual phenotype and growing features observed in the *pp2a-b'γ* mutant when grown in

moderate light and even high light conditions. However, this methodology was not able to sufficiently establish a repeatable protocol to reliably confirm or counter the proposed hypotheses. Autofluorescent signals and possible channel cross talk during the imaging sessions make it difficult to determine the success of the MitoSox labeling and thus, image processing and quantification could not be performed.

7.2. Representative Images

7.2.1. Implementation of the Original Protocol

Preliminary trials attempted to replicate the acquisition settings of the original Cvetkovska & Vanlerberghe 2012 protocol, but as can be seen in Figure 12, autofluorescent signal was detected in both the channel set up for MitoSox signal and the channel for background/autofluorescence detection in an unlabeled sample. This suggested that the autofluorescent compounds in leaf tissue, namely chlorophyll, were more strongly excited by the same laser wavelengths as the MitoSox probe than anticipated. Trials with both labeled and unlabeled, and with treated and untreated *A.thaliana* samples yielded similar images *(images not shown)*. Subsequent adjustments to the acquisition settings were then made based on the rationale that autofluorescent signal would be prevalent in all samples regardless of laser excitation wavelength. Therefore, the ideal acquisition settings would need to include a separate channel optimized for autofluorescence capture, which could then be used as background during image processing.

Nicotiana benthamiana, Wild Type, Untreated, Unlabeled, 40x	
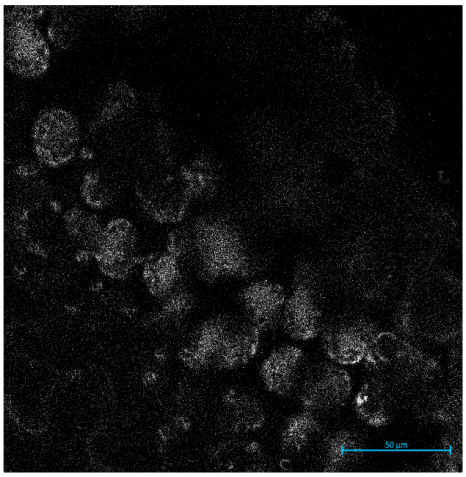	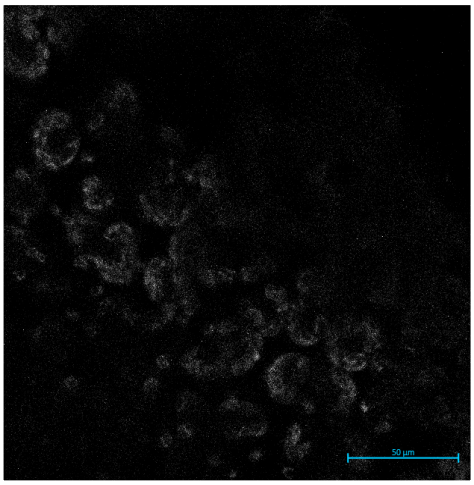
MitoSox channel Excitation: 488 nm Detection: 585-615 nm	Chlorophyll channel Excitation: 488 nm Detection: 630-650 nm
Figure 12: An unlabeled sample.	

7.2.2. Double Labeling Experiment

7.2.2.1. Negative labeling control

For subsequent trials with *A.thaliana,* a negative labeling control was established by adjusting the settings for an unlabeled sample so that no signal was captured in any of the channels of interest.

Table 4: Wild type *A.thaliana*, UV treated, Unlabeled, 20x (Figure 13)

Settings	MitoTracker channel	Chlorophyll channel	MitoSox channel
Laser:	543 nm	633 nm	488 nm
Detection:	553-606 nm	647-721 nm	500-588 nm
Gain:	834.4	550.0	630.0
Digital Gain:	1	1	1
Detector Offset:	1	3	0

Wild type *A.thaliana*, UV treated, Unlabeled, 20x

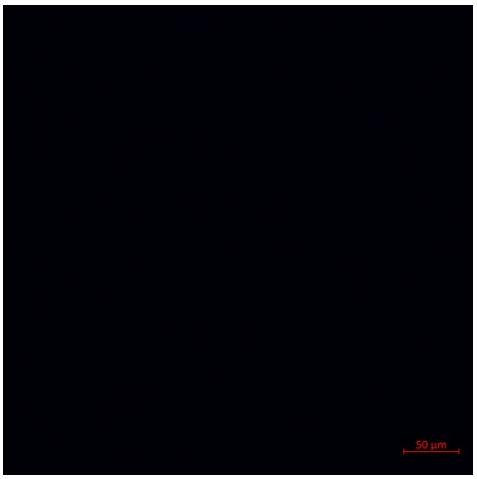

MitoTracker channel

Chlorophyll channel

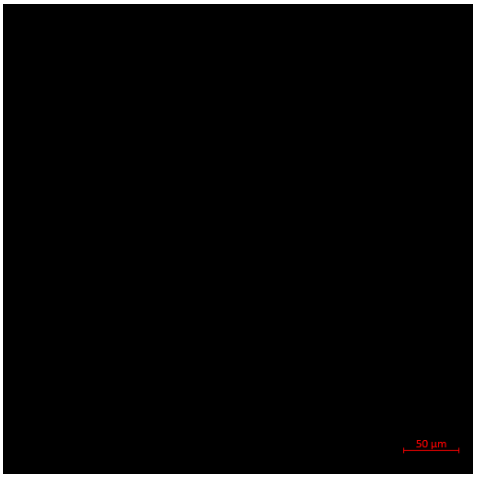

MitoSox channel

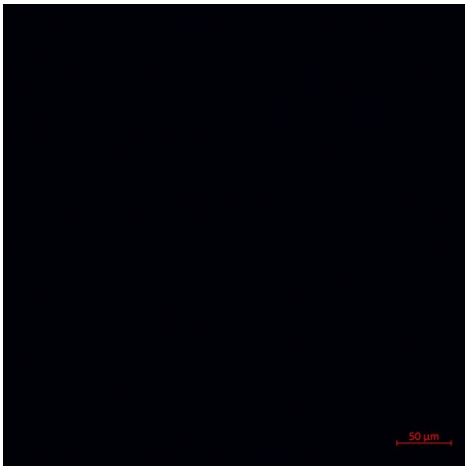

MitoTracker and MitoSox Composite

Composite

Figure 13: Negative labeling control, acquisition settings were adjusted so that no signal was captured in the channels of interest.

7.2.2.2. Positive Mitochondrial Labeling Control by MitoTracker

In order to determine if the labeling of the mitochondria by MitoSox was successful, a double labeling experiment was performed. In Figure 14, the acquisition settings are optimized in a sample labeled with MitoTracker-only as a positive labeling control.

Table 5 : Wild type *A.thaliana*, UV treated, MitoTracker, Infiltrated, 40x (Figure 14)

Settings	MitoTracker channel	Chlorophyll channel
Laser:	543 nm	633 nm
Detection:	553-606 nm	647-721 nm
Gain:	750.0	550.0
Digital Gain:	1	1
Detector Offset:	1	3

Wild type *A.thaliana*, UV treated, MitoTracker, Infiltrated, 40x

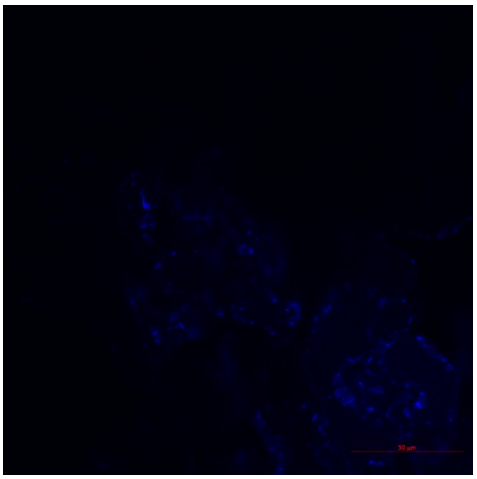

MitoTracker channel

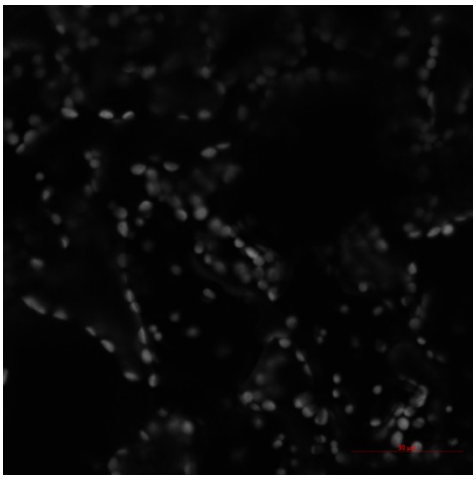

Chlorophyll channel

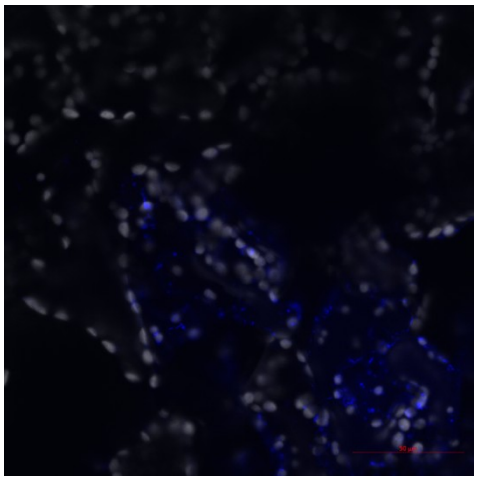

Composite

Figure 14: Positive labeling control of a Mitotracker-only labeled sample.

7.2.2.3. Double Labeled Sample to Optimize MitoSox Against MitoTracker Settings

All subsequent images were captured with the following image settings:

Table 6: Capture settings for Figures 15-20

Settings	MitoTracker channel	Chlorophyll channel	MitoSox channel
Laser:	543 nm	633 nm	488 nm
Detection:	553-606 nm	647-721 nm	588-615 nm
Gain:	913.0	659.0	913.0
Digital Gain:	1	1	1
Detector Offset:	1	2	1

MitoSox channel settings were set so as to capture signal as similar to the MitoTracker channel as possible. Image settings yielding images with less noise were favored at the cost of signal intensity.

Wild type *A.thaliana*, Untreated, MitoTracker and MitoSox, Infiltrated, 20x

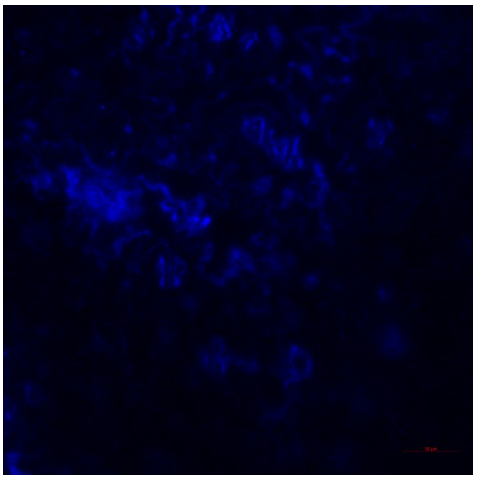

MitoTracker channel

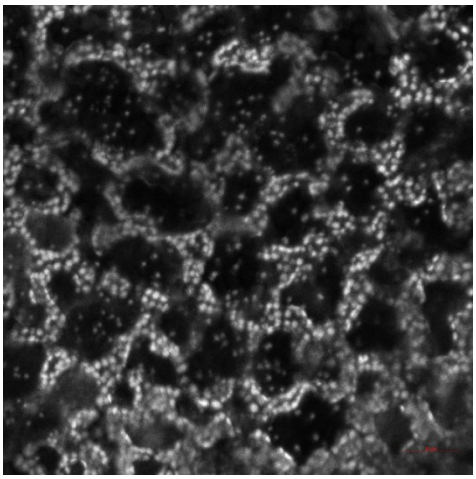

Chlorophyll channel

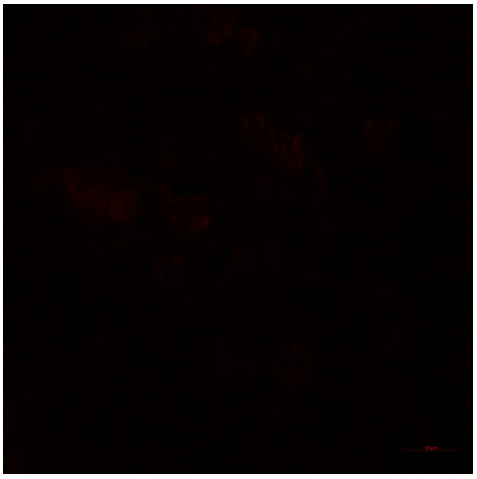

MitoSox channel

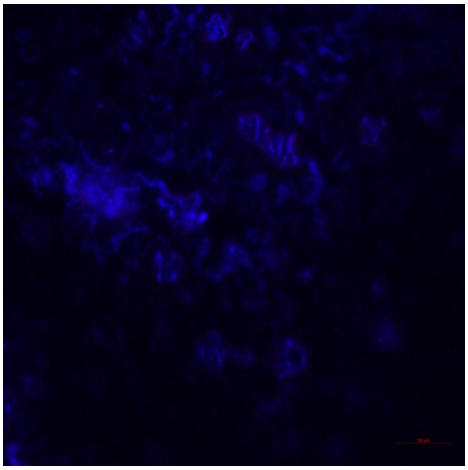

MitoTracker and MitoSox Composite

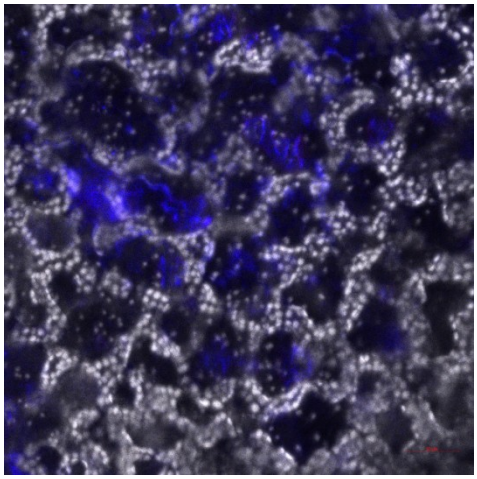

Composite

Figure 15: Double labeled sample. Image settings yielding images with less noise were favored at the cost of signal intensity.

7.2.2.4. Unlabeled Samples Imaged Using the Optimized Settings

Wild type *A.thaliana*, Unlabeled, UV Treatment, 20x

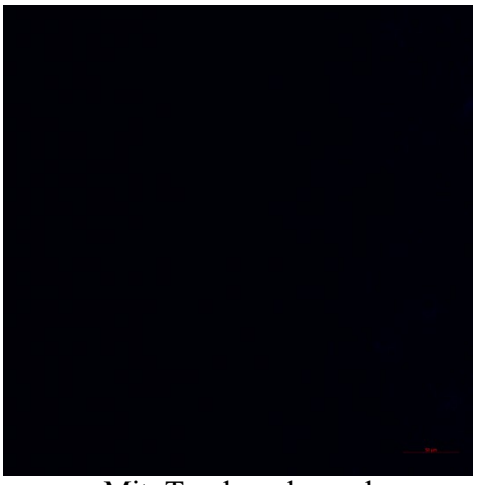

MitoTracker channel

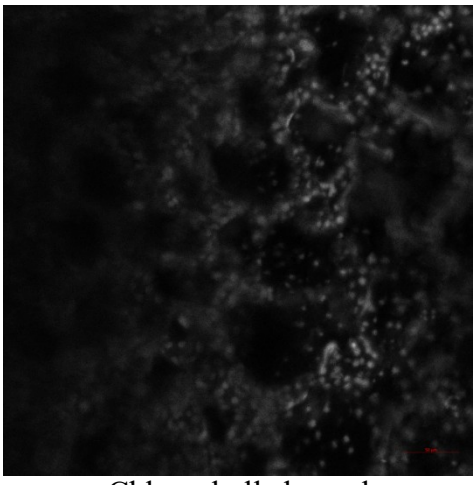

Chlorophyll channel

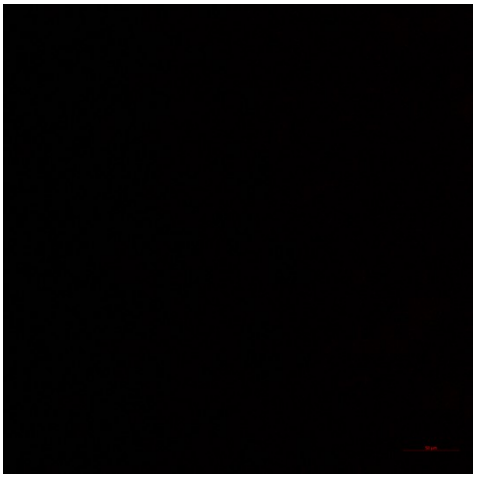

MitoSox channel

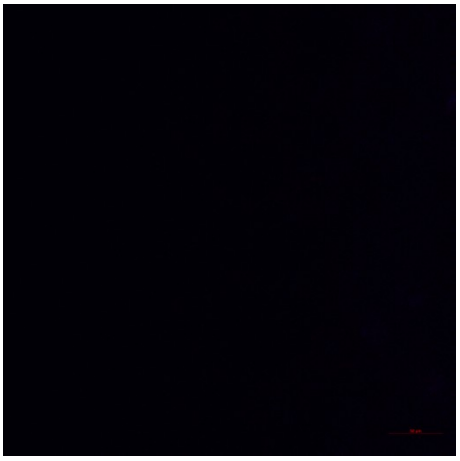

MitoTracker and MitoSox Composite

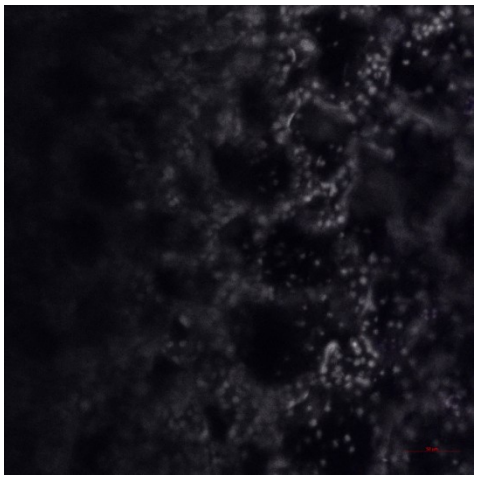

Composite

Figure 16: Unlabeled samples were imaged again using the optimized settings.

7.2.2.5. MitoTracker-Only Sample, Signal in MitoSox Channel

Wild type *A.thaliana*, MitoTracker, Infiltrated, UV Treatment, 20x

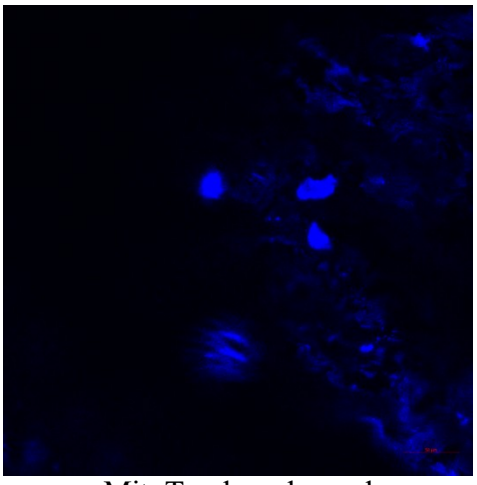

MitoTracker channel

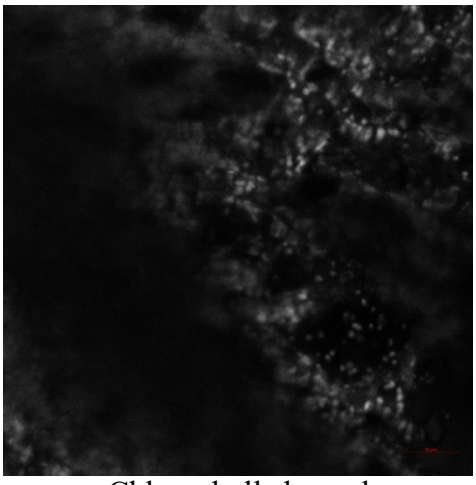

Chlorophyll channel

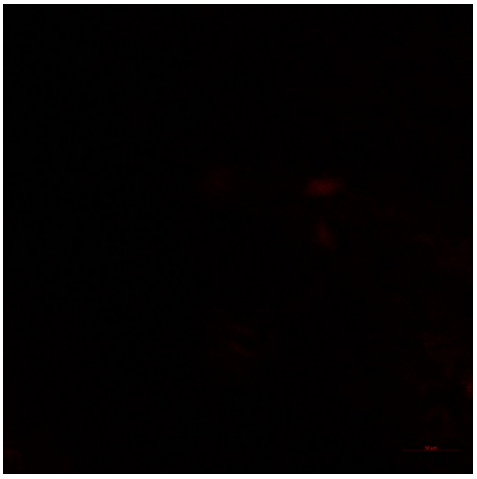

MitoSox channel

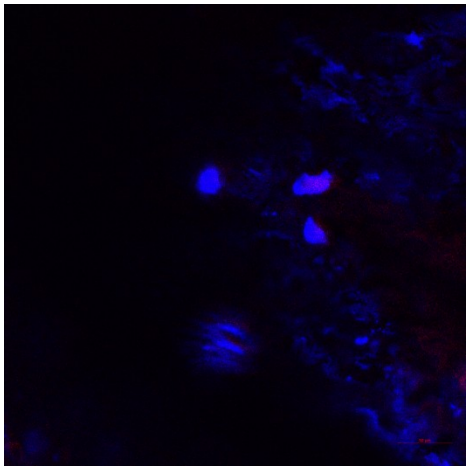

MitoTracker and MitoSox Composite

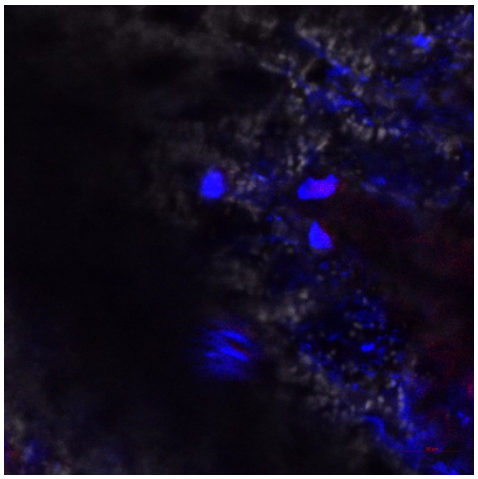

Composite

Figure 17: MitoTracker-only sample exhibits fluorescence in the MitoSox channel.

7.2.2.6. MitoSox-Only Sample, Signal in MitoTracker Channel

Wild type *A.thaliana*, MitoSox, Infiltrated, UV Treatment, 20x

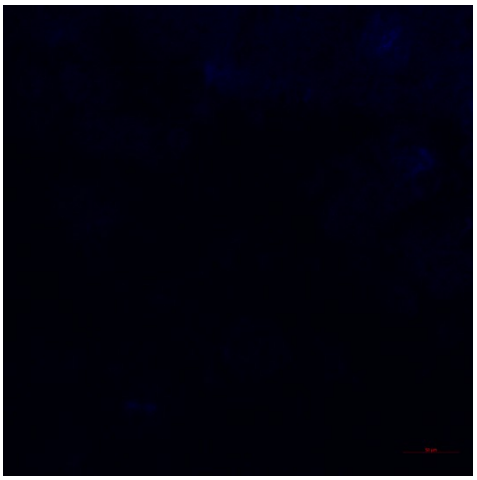

MitoTracker channel

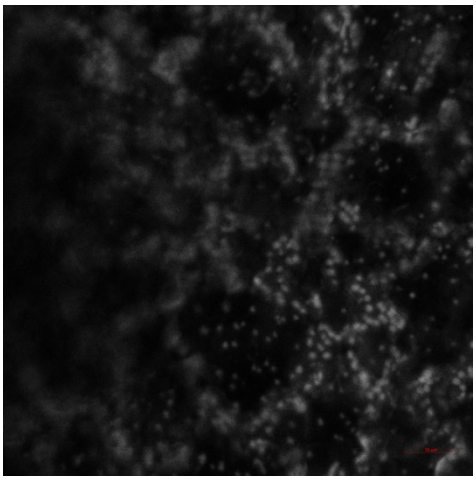

Chlorophyll channel

MitoSox channel

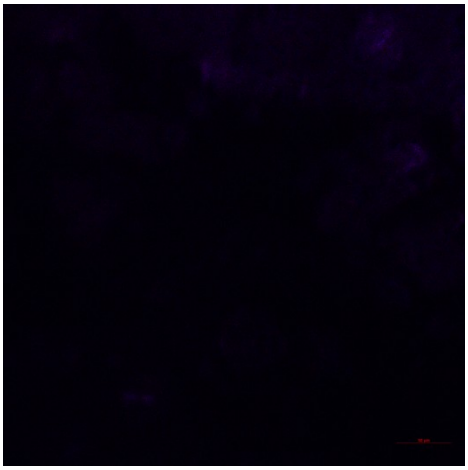

MitoTracker and MitoSox Composite

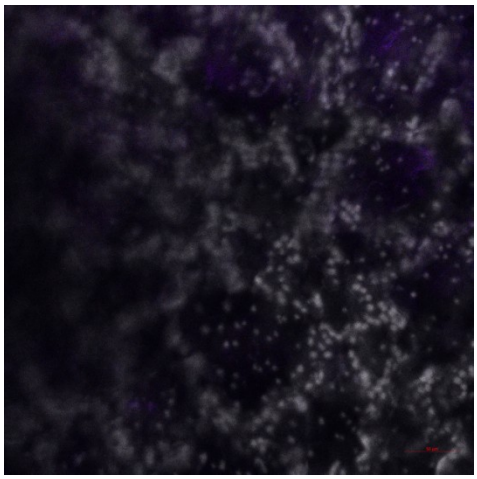

Composite

Figure 18: MitoSox-only sample exhibits fluorescence in the MitoTracker channel.

7.2.2.7. pp2a-b'γ Mitotracker-Only, Signal in MitoSox Channel

pp2a-b'γ *A.thaliana*, MitoTracker, Infiltrated, Untreated, D20x

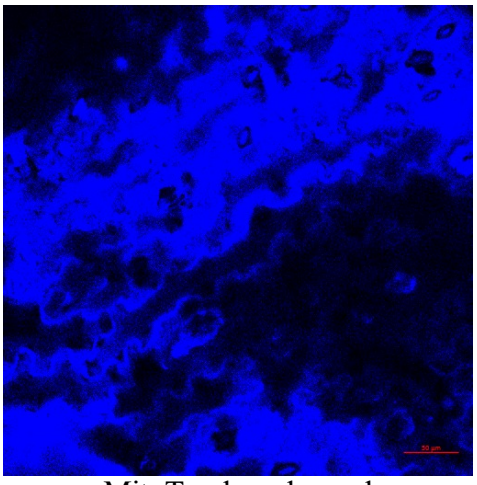

MitoTracker channel

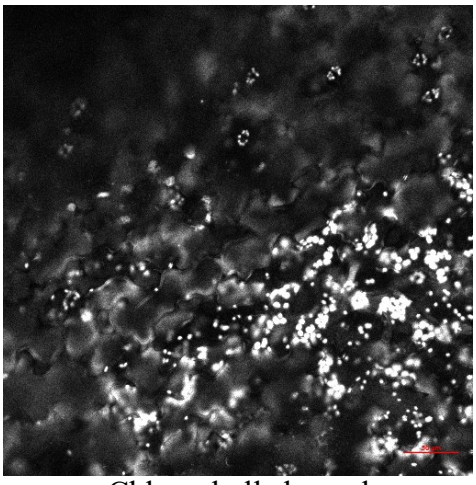

Chlorophyll channel

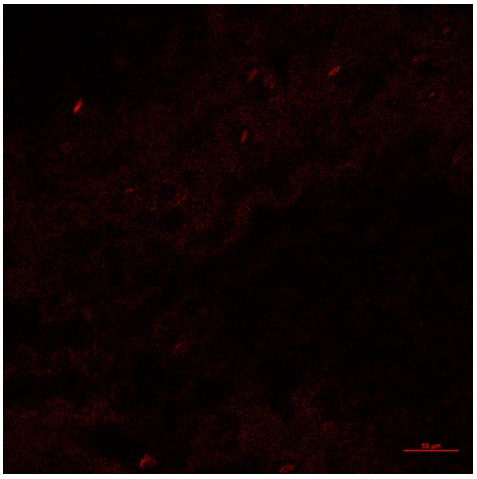

MitoSox channel

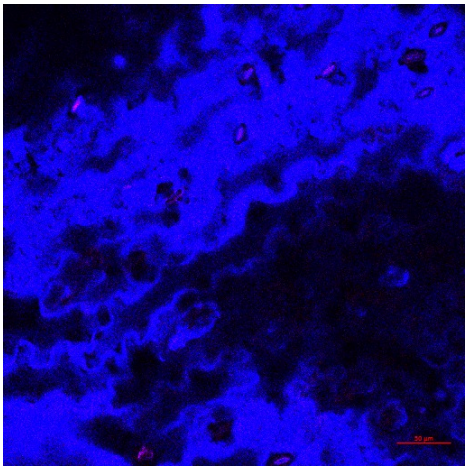

MitoTracker and MitoSox Composite

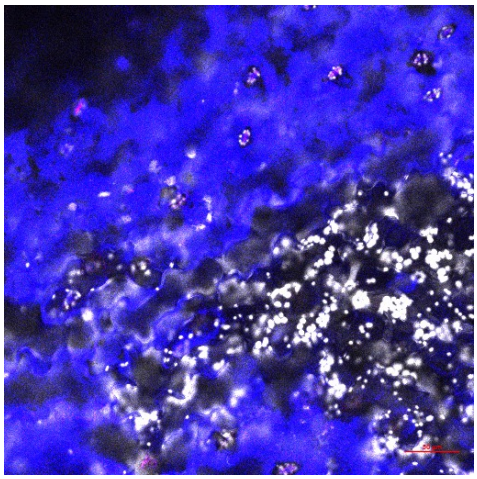

Composite

Figure 19: pp2a-b'γ Mitotracker-only with signal in MitoSox channel

7.2.2.8. pp2a-b'γ MitoSox-Only, Signal in MitoTracker Channel

pp2a-b'γ *A.thaliana*, MitoSox, Infiltrated, Untreated, 20x

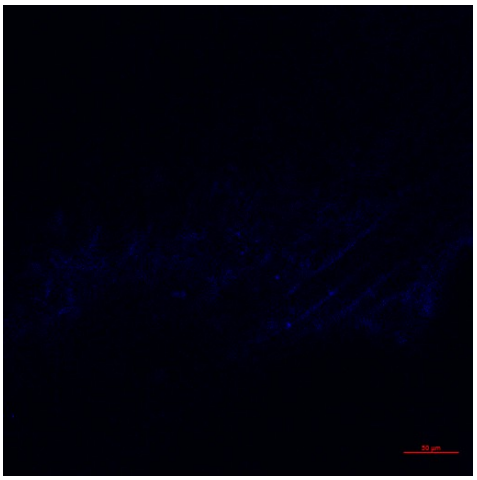

MitoTracker channel

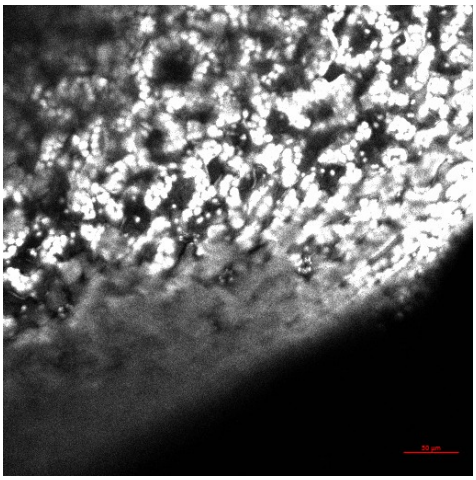

Chlorophyll channel

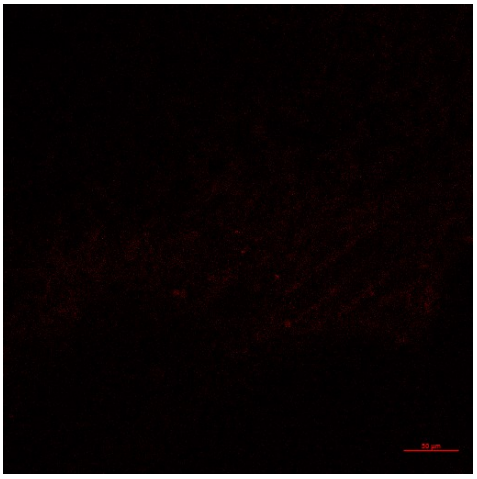

MitoSox channel

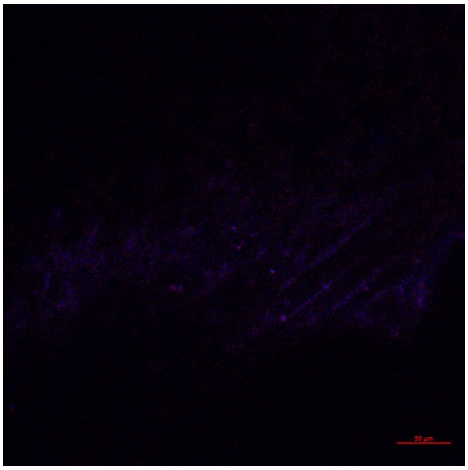

MitoTracker and MitoSox Composite

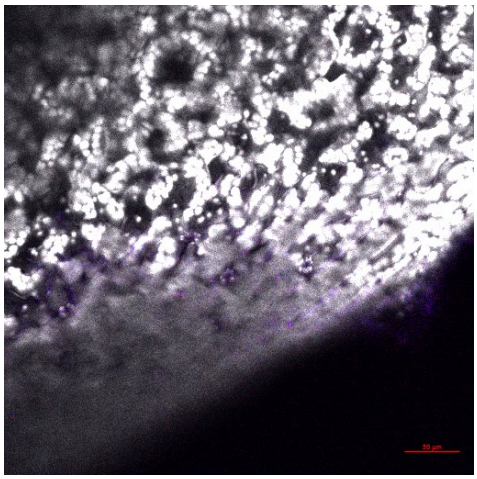

Composite

Figure 20: pp2a-b'γ MitoSox-only with signal in MitoTracker channel

7.3. Protocol Suitability in Protoplasts

The absence of the plant cell wall did not seem to improve the loading of either probe and resulting images yielded similar results as previous trials. *(Images not shown).*

7.4. Imaging aox1a, and chemically treated A. thaliana plants as Positive Controls for ROS Accumulation

To maximize the amount of ROS available to interact with MitoSox, positive controls such as *aox1a*, and chemical treatments with Antimycin A or SHAM were used. Theoretically, each one should elevate the concentration of ROS though by a different mechanism and to different degrees. Antimycin A inhibits electron transport at complex III in the mitochondrial membrane, resulting in the increased production of ROS (Maxwell et al., 1999; Vanlerberghe & McIntosh, 1997). Conversely, SHAM prevents AOX from binding to oxygen, and thus the AOX enzyme is unable to dissipate ROS, instead resulting in ROS accumulation in the mitochondria (Rasool et al., 2014; Schonbaum et al., 1971). And lastly, the *aox1a A. thaliana* mutant yielded only trace amounts of AOX1A, demonstrated a decrease in ROS dissipating pathway activity, and did not seem to recruit other antioxidant enzymes (Umbach, 2005).

However, the micrographs resulting from such samples were likewise visually indistinguishable from those of the other plant lines and between treatment groups. Because image processing could not be competently carried out on the resulting images, any comparison between the treatment groups and controls would likely suffer from a misapplication of image processing or a misinterpretation of the image processing data. *(Images not shown).*

7.5. Spectral Imaging and Linear Unmixing of aox1a Samples

Spectral imaging and linear unmixing attempts were made using samples of *aox1a.* The resulting images were plagued by noise and both manual selection of representative pixels of each fluorophore, as well as computer suggested ones were not able to

satisfactorily separate autofluorescence from MitoSox nor MitoTracker signals in each channel.

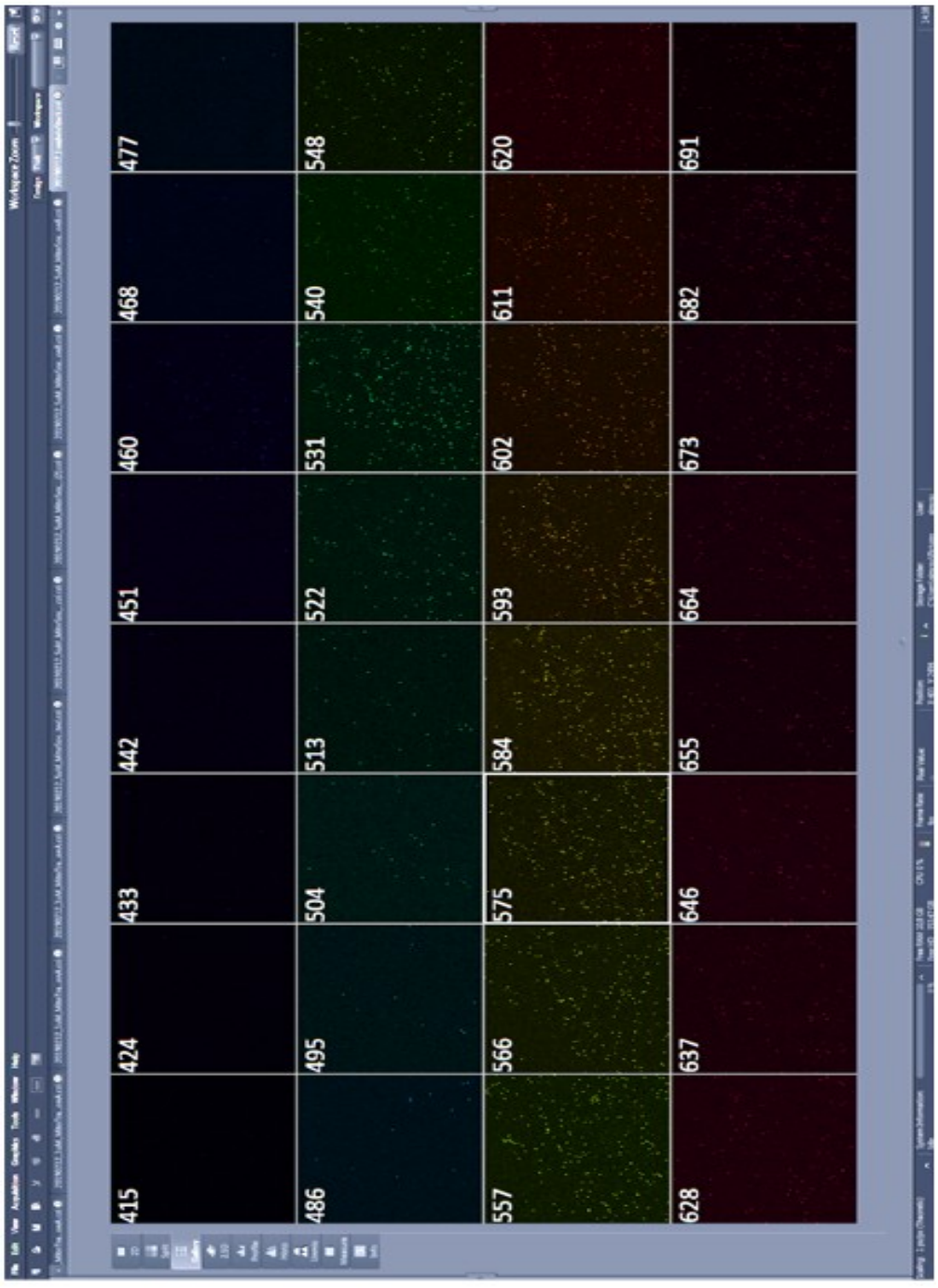

Figure 21: Lambda stack of double labeled sample.

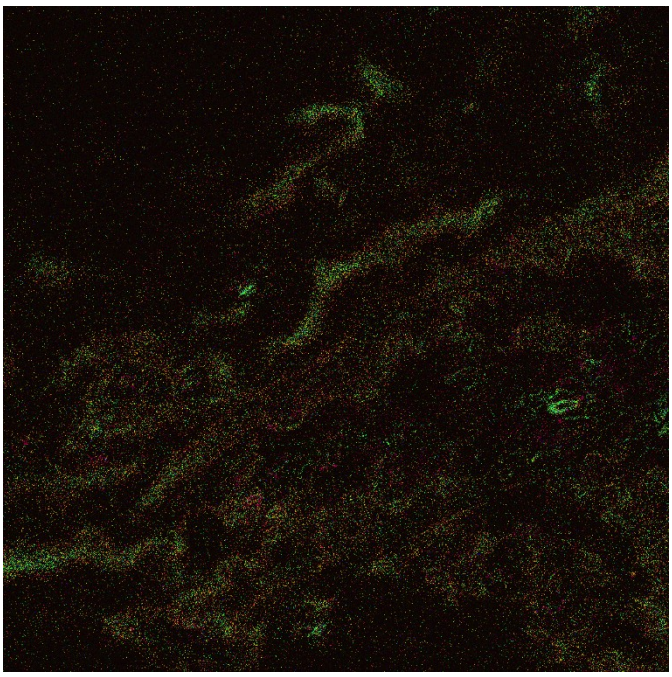

Figure 22: Computer generated ACE unmixed image.

8. Discussion

8.1. Reflection of Study Design and Results

Despite attempts to minimize channel crosstalk and the excitation of autofluorescent compounds, the protocol could not be satisfactorily optimized and consistently implemented during the course of this thesis project. The signals detected in the MitoSox channel, and even in the MitoTracker channel, could not be confidently attributed to the excitation of the desired probe alone, since unexpected fluorescence was detected in both unlabeled samples and single-probe labeled samples. The signals captured and their respective images could be due the excitation of autofluorescent compounds, poor probe loading results, channel crosstalk, or some combination thereof.

This thesis project also examined whether factors such as the plant species, type of mutation, age of the plant, age of the leaf, presence of a plant cell wall, treatment type, probe loading methods, and/or incubation parameters could be adjusted to improve image results. Unfortunately, these parameters don't appear to significantly improve nor harm the imaging results, so the parameters listed in the final protocol were selected based on other criteria, such as efficiency, availability, and ease of application.

8.2. Critical Evaluation of ROS Quantification Methodologies

As a natural byproduct of cellular metabolism, a prominent cellular signaling molecule, and a potentially damaging oxidative chemical compounds, researchers have long been interested in understanding the many functions of metabolic ROS. However, current quantification methods are subject to numerous difficulties, in both application and in achieving accurate results. ROS tend to be highly volatile, and as they are so ubiquitous, the cellular system demonstrates numerous elegant mechanisms which dissipate ROS quickly. Proposed to be the cause of many metabolic related diseases, when an organism is lacking these mechanisms, if it is not lethal, the cells suffer significantly. Additionally, ROS concentration is easily impacted by stress, disease, and damage, and thus the data gathered from research studies are inherently biased by any collection, treatment, and processing methods. In an attempt to address these concerns, researchers have relied on the use of MitoSox to make the quantification of ROS possible, however, while it has its merits, the use of MitoSox also has numerous pitfalls.

In order to quantify ROS using MitoSox, fresh tissue samples must be harvested, labeled, and imaged within a short time period. Ideally, any signal that arises from labeling could be attributed to the presence of ROS in the mitochondria, and because un-oxidized MitoSox (DHE) is non fluorescent, the amount of signal captured would be directly proportional to the amount of ROS present. Through the application of image processing, the amount of signal could be then be compared relative to other labeled samples and with a large enough sample size, it would be possible to statistically compare the results.

However, the use of MitoSox as a quantitative measure has been heavily disputed throughout the years. In 1998, Benov *et al.* determined that while DHE could be oxidized by O_2^- into fluorescent 2-OH-E, it was not stoichiometrically proportionate and would underrepresent the amount of ROS present. Then, over the next decade, researchers disputed about whether DHE could oxidize into at least one other fluorescent product with distinctly different excitation and emission peaks from 2-OH-E (Zhao et al., 2003). While the laboratory of Michalski *et al* maintains that 2-OH-E is the only product formed by the oxidation of DHE by O_2^-, MitoSox still exhibits nonspecific

oxidation by other oxidative compounds (Michalski, Michalowski, Sikora, Zielonka, & Kalyanaraman, 2014). The generation of multiple fluorescent products would complicate any quantitative attempts because the amount of fluorescence imaged could be misrepresented by the other products (Zhao et al., 2003).

This tolls heavily against the continued use of MitoSox as a ROS specific probe, and is only ameliorated by technological advancements which give microscopists the ability to finely tune instrument detection settings to capture the emission of 2-OH-E (Zielonka & Kalyanaraman, 2010). By being able to specifically select the detection range of a microscope, researchers are able to exclude some of the emission resulting from nonspecific oxidation of MitoSox. Thus, in a carefully designed experiment that utilizes the same equipment, sample preparation techniques, and imaging settings, researchers are able to make justifiable quantitative comparisons relative to other the samples collected in the same experiment. In this manner, careful application of image processing techniques can yield statistically valid information. Therefore, though this approach is limited as a stand-alone methodology, it is valuable as a qualitative support and for visualizing abstract cellular concepts.

8.3. Significance

For plants, being able to respond and acclimate to environmental stress is critical for continued growth and proliferation. By maintaining the balance of ROS within the cell, plants are able to adapt to the current environmental conditions and may even be able to adapt more quickly to additional stressors. While it may not perfectly represent natural conditions, understanding how the mechanisms in this pathway interact when subjected to a particular stress, such as UV-B radiation, allows researchers to study specific pathway interactions more thoroughly.

In order to study plant tissues microscopically, it is important to anticipate how autofluorescent compounds will affect the final image results. In ideal situations, with good microscopy practices and image data analysis techniques, autofluorescent signal can be separated from the signals of interest, to generate strong and unbiased data. By utilizing both positive and negative controls for their probes, researchers can establish the proper microscopy capture settings for their samples, improve the reproducibility of their work, and perform better image analysis. To achieve this purpose, many tools,

strategies, and methods have been developed in order to capture the most accurate data from samples. However, as demonstrated by this Master's Thesis, such applications still have their limitations. Here, the apparent signal cross talk between autofluorescent compounds and the labeling probes could not be eliminated by changing the methodology, nor by image processing, thus preventing any quantitative or qualitative data collection. These difficulties were compounded by the unforgiving nature of imaging fresh tissue samples as well as what is known about the volatile qualities of the ROS therein.

Nonetheless, ROS are prolific and essential metabolic and cell signaling components, not only in plants, but across the biological sciences. Therefore, research efforts on their study will continue to be a priority in the scientific community. As new techniques and technology improves our understanding of the delicate and diverse role of cellular ROS, new insights into its functions will untangle other mysteries as well.

9. Acknowledgments

Many thanks to . . .

Dr. Saijaliisa Kangasjärvi

Dr. Jesús Pascual Vázquez

Sara Alegre García

Dr. Moona Rahikainen

Dr. Guido Durian

Ilona Varjus

Dr. Martina Angeleri

Zsófia Winter

Ciarán Butler-Hallissey

Dr. Diana Toivola

Joanna Pylvänäinen

Maritta Löytömäki

Elena Tcarenkova

Uruj Fatima Sarwar

Turku Center for Biotechnology Cell Imaging Core

Everyone in the Turku Molecular Plant Biology Lab and their collaborators

My professors and classmates

My friends and family across the globe

Thank You!

10. References

Atkinson, N. J., & Urwin, P. E. (2012). REVIEW The Interaction of plant biotic and abiotic stresses: from genes to the field. *Journal of Experimental Botany*. https://doi.org/10.1093/jxb/err313

Bakeeva, L. E., Grinius, L. L., Jasaitis, A. A., Kuliene, V. V., Levitsky, D. O., Liberman, E. A., … Skulachev, V. P. (1970). Conversion of biomembrane-produced energy into electric form. II. Intact mitochondria. *BBA - Bioenergetics*. https://doi.org/10.1016/0005-2728(70)90154-4

Baxter, A., Mittler, R., & Suzuki, N. (2014). ROS as key players in plant stress signalling. *Journal of Experimental Botany*, *65*(5), 1229–1240. https://doi.org/10.1093/jxb/ert375

Baxter, C. J., Redestig, H., Schauer, N., Repsilber, D., Patil, K. R., Nielsen, J., … Sweetlove, L. J. (2007). The metabolic response of heterotrophic Arabidopsis cells to oxidative stress. *Plant Physiology*, *143*(1), 312–325. https://doi.org/10.1104/pp.106.090431

Benov, L., Sztejnberg, L., & Fridovich, I. (1998). Critical evaluation of the use of hydroethidine as a measure of superoxide anion radical. *Free Radical Biology and Medicine*. https://doi.org/10.1016/S0891-5849(98)00163-4

Brown, B. A., & Jenkins, G. I. (2008). UV-B signaling pathways with different fluence-rate response profiles are distinguished in mature Arabidopsis leaf tissue by requirement for UVR8, HY5, and HYH. *Plant Physiology*, *146*(2), 576–588. https://doi.org/10.1104/pp.107.108456

Cho, U. S., & Xu, W. (2007). Crystal structure of a protein phosphatase 2A heterotrimeric holoenzyme. *Nature*, *445*(7123), 53–57. https://doi.org/10.1038/nature05351

Cvetkovska, M., & Vanlerberghe, G. C. (2012). Alternative oxidase modulates leaf mitochondrial concentrations of superoxide and nitric oxide. *New Phytologist*. https://doi.org/10.1111/j.1469-8137.2012.04166.x

Cvetkovska, M., & Vanlerberghe, G. C. (2015). *Chapter 18: In Planta Analysis of Leaf Mitochondrial Superoxide and Nitric Oxide* (James Whelan & Monika W. Murcha, eds.).

Diaspro, A., Bianchini, P., Vicidomini, G., Faretta, M., Ramoino, P., & Usai, C. (2006). Multi-photon excitation microscopy. *BioMedical Engineering OnLine*, *5*(1), 36. https://doi.org/10.1186/1475-925X-5-36

Dickinson, M. E., & Davidson, M. W. (n.d.-a). ZEISS Microscopy Online Campus | Introduction to Spectral Imaging. Retrieved May 17, 2019, from http://zeiss-campus.magnet.fsu.edu/print/spectralimaging/introduction-print.html

Dickinson, M. E., & Davidson, M. W. (n.d.-b). ZEISS Microscopy Online Campus | Introduction to Spectral Imaging. Retrieved February 7, 2019, from http://zeiss-campus.magnet.fsu.edu/articles/spectralimaging/introduction.html

Dihydroethidium (Hydroethidine) - Thermo Fisher Scientific. (n.d.). Retrieved February 4, 2019, from https://www.thermofisher.com/order/catalog/product/D1168

Dikalov, S. I., & Harrison, D. G. (2014). REVIEW Methods for detection of mitochondrial and cellular reactive oxygen species. *Antioxidants & Redox Signaling*, *20*(2), 372–382. https://doi.org/10.1089/ars.2012.4886

Eckardt, N. A., Snyder, G. W., Portis, A. R., Orgen, W. L., & Orgen, W. L. (1997). Growth and photosynthesis under high and low irradiance of Arabidopsis thaliana antisense mutants with reduced ribulose-1,5-bisphosphate carboxylase/oxygenase activase content. *Plant Physiology*, *113*(2), 575–586. Retrieved from http://www.ncbi.nlm.nih.gov/pubmed/9046598

File:Antimycin A1 Structural Formula V1.svg - Wikimedia Commons. (n.d.). Retrieved May 17, 2019, from https://commons.wikimedia.org/wiki/File:Antimycin_A1_Structural_Formula_V1.svg

File:Salicylhydroxamic acid.png - Wikimedia Commons. (n.d.). Retrieved May 17, 2019, from https://commons.wikimedia.org/wiki/File:Salicylhydroxamic_acid.png

File:ZEISS LSM 880 with Airyscan (14657209838).jpg - Wikimedia Commons. (n.d.). Retrieved May 17, 2019, from https://commons.wikimedia.org/wiki/File:ZEISS_LSM_880_with_Airyscan_(14657209838).jpg

Foyer, C. H., Leiandais, M., Foyer, K. J. K., Leiandais, C. H., & Kunert, M. (n.d.). *REVIEW Photooxidative stress in plants*.

Foyer, C. H., & Noctor, G. (2003). REVIEW Redox sensing and signalling associated with reactive oxygen in chloroplasts, peroxisomes and mitochondria. *Physiologia Plantarum*, *119*(3), 355–364. https://doi.org/10.1034/j.1399-3054.2003.00223.x

Foyer, C. H., Rasool, B., Davey, J. W., & Hancock, R. D. (2016). REVIEW Cross-Tolerance to biotic and abiotic stresses in plants: A focus on resistance to aphid infestation. *Journal of Experimental Botany*. https://doi.org/10.1093/jxb/erw079

Goodwin, R. H. (1953). Fluorescent Substances in Plants. *Annual Review of Plant Physiology*, *4*(1), 283–304. https://doi.org/10.1146/annurev.pp.04.060153.001435

Gupta, K. J., Shah, J. K., Brotman, Y., Jahnke, K., Willmitzer, L., Kaiser, W. M., … Igamberdiev, A. U. (2012). Inhibition of aconitase by nitric oxide leads to induction of the alternative oxidase and to a shift of metabolism towards biosynthesis of amino acids. *Journal of Experimental Botany*, *63*(4), 1773–1784. https://doi.org/10.1093/jxb/ers053

Igamberdiev, A. U., & Eprintsev, A. T. (2016). Organic Acids: The Pools of Fixed Carbon Involved in Redox Regulation and Energy Balance in Higher Plants. *Frontiers in Plant Science*. https://doi.org/10.3389/fpls.2016.01042

Kalve, S., Fotschki, J., Beeckman, T., Vissenberg, K., & Beemster, G. T. S. (2014). Three-dimensional patterns of cell division and expansion throughout the development of Arabidopsis thaliana leaves. *Journal of Experimental Botany*, *65*(22), 6385–6397. https://doi.org/10.1093/jxb/eru358

Knight, H., & Knight, M. R. (2001). REVIEW Abiotic stress signalling pathways: specificity and cross-talk. *Trends in Plant Science*, *6*(6), 262–267. https://doi.org/10.1016/S1360-1385(01)01946-X

Kodama, Y. (2016). Time gating of chloroplast autofluorescence allows clearer fluorescence imaging in planta. *PLoS ONE*. https://doi.org/10.1371/journal.pone.0152484

Konert, G. (2014). *PP2A: AT THE CROSSROADS BETWEEN GROWTH AND DEFENCE IN PLANTS*.

Konert, G., Trotta, A., Kouvonen, P., Rahikainen, M., Durian, G., Blokhina, O., … Kangasjärvi, S. (2014). Protein phosphatase 2A (PP2A) regulatory subunit B′γ interacts with cytoplasmic ACONITASE 3 and modulates the abundance of AOX1A and AOX1D in *Arabidopsis thaliana*. *New Phytologist*, *205*(3), 1250–1263. https://doi.org/10.1111/nph.13097

Koornneef, M., & Meinke, D. (2010). REVIEW The development of Arabidopsis as a model plant. *The Plant Journal*, *61*(6), 909–921. https://doi.org/10.1111/j.1365-313X.2009.04086.x

Li, S., Mhamdi, A., Trotta, A., Kangasjärvi, S., & Noctor, G. (2014). The protein phosphatase subunit PP2A-B′γ is required to suppress day length-dependent pathogenesis responses triggered by intracellular oxidative stress. *New Phytologist*, *202*(1), 145–160. https://doi.org/10.1111/nph.12622

Liao, X., & Butow, R. A. (1993). RTG1 and RTG2: Two yeast genes required for a novel path of communication from mitochondria to the nucleus. *Cell*, *72*(1), 61–71. https://doi.org/10.1016/0092-8674(93)90050-Z

Lichtenthaler, H. K. (1995). REVIEW Vegetation Stress: an Introduction to the Stress Concept in Plants. *Journal of Plant Physiology*. https://doi.org/10.1016/s0176-1617(96)80287-2

Maxwell, D. P., Wang, Y., & McIntosh, L. (1999). The alternative oxidase lowers mitochondrial reactive oxygen production in plant cells. *Proceedings of the National Academy of Sciences of the United States of America*, *96*(14), 8271–8276. Retrieved from http://www.ncbi.nlm.nih.gov/pubmed/10393984

Michalski, R., Michalowski, B., Sikora, A., Zielonka, J., & Kalyanaraman, B. (2014). On the use of fluorescence lifetime imaging and dihydroethidium to detect superoxide in intact animals and ex vivo tissues: a reassessment. *Free Radical Biology & Medicine*, *67*, 278–284. https://doi.org/10.1016/j.freeradbiomed.2013.10.816

MitoSOX Red Mitochondrial Superoxide Indicator, for live-cell imaging - Thermo Fisher Scientific. (n.d.). Retrieved February 4, 2019, from https://www.thermofisher.com/order/catalog/product/M36008

MitoTracker Orange CMTMRos - Special Packaging - Thermo Fisher Scientific. (n.d.). Retrieved May 17, 2019, from https://www.thermofisher.com/order/catalog/product/M7510?SID=srch-srp-M7510

Mittler, R. (2006). OPINION/REVIEW Abiotic stress, the field environment and stress combination. *Trends in Plant Science*, *11*(1), 15–19. https://doi.org/10.1016/J.TPLANTS.2005.11.002

Møller, I. M. (2001). REVIEW PLANT M ITOCHONDRIA AND OXIDATIVE S TRESS : Electron Transport, NADPH Turnover, and Metabolism of Reactive Oxygen Species. *Annual Review of Plant Physiology and Plant Molecular Biology*, *52*(1), 561–591. https://doi.org/10.1146/annurev.arplant.52.1.561

Moore, A. L., & Siedow, J. N. (1991). The regulation and nature of the cyanide-resistant alternative oxidase of plant mitochondria. *Biochimica et Biophysica Acta (BBA) - Bioenergetics*, *1059*(2), 121–140. https://doi.org/10.1016/S0005-2728(05)80197-5

Moorhead, G. B. G., De Wever, V., Templeton, G., & Kerk, D. (2009). Evolution of protein phosphatases in plants and animals. *Biochemical Journal*, *417*(2), 401–409. https://doi.org/10.1042/BJ20081986

Müller-Xing, R., Xing, Q., & Goodrich, J. (2014). REVIEW Footprints of the sun: memory of UV and light stress in plants. *Frontiers in Plant Science*, *5*, 474. https://doi.org/10.3389/fpls.2014.00474

Nawkar, G. M., Maibam, P., Park, J. H., Sahi, V. P., Lee, S. Y., & Kang, C. H. (2013). REVIEW UV-Induced cell death in plants. *International Journal of Molecular Sciences*, *14*(1), 1608–1628. https://doi.org/10.3390/ijms14011608

Nicolas George. (2004). Spinning Disk vs. Laser-Scanning Confocal Microscopes | Features | Oct 2004 | Photonics Spectra. Retrieved February 23, 2019, from https://www.photonics.com/Articles/Spinning_Disk_vs_Laser-Scanning_Confocal/a20129

Poot, M., Zhang, Y. Z., Krämer, J. A., Wells, K. S., Jones, L. J., Hanzel, D. K., … Haugland, R. P. (1996). Analysis of mitochondrial morphology and function with novel fixable fluorescent stains. *Journal of Histochemistry and Cytochemistry*. https://doi.org/10.1177/44.12.8985128

Product Info: Fluorescent probes for plant imaging Invitrogen tools for plant cell biology. (n.d.). Retrieved from www.invitrogen.com

Rahikainen, M. (2018). *Moona Rahikainen: PLANT DEFENCE AND STRESS ACCLIMATION: REGULATION BY PROTEIN PHOSPHATASE 2A*. Retrieved from http://urn.fi/URN:ISBN:978-951-29-7271-5

Rahikainen, M., Pascual, J., Alegre, S., Durian, G., & Kangasjärvi, S. (2016). REVIEW PP2A Phosphatase as a Regulator of ROS Signaling in Plants. *Antioxidants*. https://doi.org/10.3390/antiox5010008

Rasool, B., Karpinska, B., Konert, G., Durian, G., Denessiouk, K., Kangasjärvi, S., & Foyer, C. H. (2014). Effects of light and the regulatory B-subunit composition of protein phosphatase 2A on the susceptibility of Arabidopsis thaliana to aphid (Myzus persicae) infestation. *Frontiers in Plant Science*, *5*, 405. https://doi.org/10.3389/fpls.2014.00405

Rejeb, I. Ben, Pastor, V., & Mauch-Mani, B. (2014). REVIEW Plant Responses to Simultaneous Biotic and Abiotic Stress: Molecular Mechanisms. *Plants (Basel, Switzerland)*, *3*(4), 458–475. https://doi.org/10.3390/plants3040458

Rizhsky, L., Liang, H., Shuman, J., Shulaev, V., Davletova, S., & Mittler, R. (2004). When defense pathways collide. The response of Arabidopsis to a combination of drought and heat stress. *Plant Physiology*, *134*(4), 1683–1696. https://doi.org/10.1104/pp.103.033431

Robinson, K. M., Janes, M. S., Pehar, M., Monette, J. S., Ross, M. F., Hagen, T. M., … Beckman, J. S. (2006). *Selective fluorescent imaging of superoxide in vivo using ethidium-based probes* (Vol. 103). Retrieved from www.pnas.orgcgidoi10.1073pnas.0601945103

Schonbaum, G. R., Bonner, W. D., Storey, B. T., Bahr, J. T., & Bahr, J. T. (1971). Specific inhibition of the cyanide-insensitive respiratory pathway in plant mitochondria by hydroxamic acids. *Plant Physiology*, *47*(1), 124–128. https://doi.org/10.1104/pp.47.1.124

Selinski, J., Hartmann, A., Deckers-Hebestreit, G., Day, D. A., Whelan, J., & Scheibe, R. (2018). Alternative Oxidase Isoforms Are Differentially Activated by Tricarboxylic Acid Cycle Intermediates. *Plant Physiology*, *176*(2), 1423–1432. https://doi.org/10.1104/pp.17.01331

Trotta, A., Rahikainen, M., Konert, G., Finazzi, G., & Kangasjärvi, S. (2014). REVIEW Signalling crosstalk in light stress and immune reactions in plants. *Philosophical Transactions of the Royal Society of London. Series B, Biological Sciences*, *369*(1640), 20130235. https://doi.org/10.1098/rstb.2013.0235

Trotta, A., Wrzaczek, M., Scharte, J., Tikkanen, M., Konert, G., Rahikainen, M., … Kangasjärvi, S. (2011). Regulatory subunit B'gamma of protein phosphatase 2A prevents unnecessary defense reactions under low light in Arabidopsis. *Plant Physiology*, *156*(3), 1464–1480. https://doi.org/10.1104/pp.111.178442

Umbach, A. L. (2005). Characterization of Transformed Arabidopsis with Altered Alternative Oxidase Levels and Analysis of Effects on Reactive Oxygen Species in Tissue. *PLANT PHYSIOLOGY*, *139*(4), 1806–1820. https://doi.org/10.1104/pp.105.070763

Vanlerberghe, G. C., & McIntosh, L. (1997). REVIEW ALTERNATIVE OXIDASE: From Gene to Function. *Annual Review of Plant Physiology and Plant Molecular Biology*, *48*(1), 703–734. https://doi.org/10.1146/annurev.arplant.48.1.703

Verniquet, F., Gaillard, J., Neuburger, M., & Douce, R. (1991). Rapid inactivation of plant aconitase by hydrogen peroxide. *The Biochemical Journal*, *276 (Pt 3)*(Pt 3), 643–648. https://doi.org/10.1042/bj2760643

Vishwakarma, A., Bashyam, L., Senthilkumaran, B., Scheibe, R., & Padmasree, K. (2014). Physiological role of AOX1a in photosynthesis and maintenance of cellular redox homeostasis under high light in Arabidopsis thaliana. *Plant Physiology and Biochemistry*, *81*, 44–53. https://doi.org/10.1016/J.PLAPHY.2014.01.019

Wu, F.-H., Shen, S.-C., Lee, L.-Y., Lee, S.-H., Chan, M.-T., & Lin, C.-S. (2009). Tape-Arabidopsis Sandwich - a simpler Arabidopsis protoplast isolation method. *Plant Methods*, *5*, 16. https://doi.org/10.1186/1746-4811-5-16

Zarkovic, J., Anderson, S. L., & Rhoads, D. M. (2005). A reporter gene system used to study developmental expressionof alternative oxidase and isolate mitochondrial retrograde regulationmutants in Arabidopsis. *Plant Molecular Biology*, *57*(6), 871–888. https://doi.org/10.1007/s11103-005-3249-0

Zhao, H., Kalivendi, S., Zhang, H., Joseph, J., Nithipatikom, K., Vásquez-Vivar, J., & Kalyanaraman, B. (2003). Superoxide reacts with hydroethidine but forms a fluorescent product that is distinctly different from ethidium: Potential implications in intracellular fluorescence detection of superoxide. *Free Radical Biology and Medicine*. https://doi.org/10.1016/S0891-5849(03)00142-4

Zhou, X., Carranco, R., Vitha, S., & Hall, T. C. (2005). The dark side of green fluorescent protein. *New Phytologist*, *168*(2), 313–322. https://doi.org/10.1111/j.1469-8137.2005.01489.x

Zielonka, J., & Kalyanaraman, B. (2010). REVIEW Hydroethidine- and MitoSOX-derived red fluorescence is not a reliable indicator of intracellular superoxide formation: another inconvenient truth. *Free Radical Biology & Medicine*, *48*(8), 983–1001. https://doi.org/10.1016/j.freeradbiomed.2010.01.028

11. List of Figures

12. Signatures

Diana Toivola

Sara Alegre García

Jesús Pascual Vázquez

Saijaliisa Kangasjäarvi

Allison McGuire